FUNCTIONALIZATION OF NANOMATERIAL: APPLIED FOR ENVIRONMENTAL REMEDIATION

A THESIS SUBMITTED TO
THE GRADUATE SCHOOL OF NATURAL AND APPLIED SCIENCES
OF
MIDDLE EAST TECHNICAL UNIVERSITY

BY

EDA ALEMDAR

IN PARTIAL FULFILLMENT OF THE REQUIREMENTS
FOR
THE DEGREE OF MASTER OF SCIENCE
IN
CHEMISTRY

SEPTEMBER 2017

Approval of the Thesis

FUNCTIONALIZATION OF NANOMATERIAL: APPLIED FOR ENVIRONMENTAL REMEDIATION

Submitted by **EDA ALEMDAR** in partial fulfillment of the requirements for the degree of **Master of Science in Chemistry Department. Middle East Technical University** by.

Prof. Dr. Gülbin Dural Ünver
Dean. Graduate School of **Natural and Applied Sciences** _____

Prof. Dr. Cihangir Tanyeli
Head of Department, **Chemistry** _____

Prof. Dr. Semra TUNCEL
Supervisor, **Chemistry Department. METU** _____

Prof. Dr. Gülsün Gökağaç**. METU**
Co-Supervisor, **Chemistry Department. METU** _____

Examining Committee Members:

Prof. Dr. Ali Gökmen
Chemistry Dept., METU _____

Prof. Dr. Semra Tuncel
Chemistry Dept., METU _____

Prof. Dr. Gülsün Gökağaç
Chemistry Dept., METU _____

Assis. Prof. Dr. Gülay Ertaş
Chemistry Dept., METU _____

Prof. Dr. Gülen Güllü
Environmental Engineering Dept., Hacettepe University _____

Date: 20 September 2017

.

I hereby declare that all information in this document has been obtained and presented in accordance with academic rules and ethical conduct. I also declare that as required by these rules and conduct. I have fully cited and referenced all materials and results that are not original to this work.

Name, Lastname: Eda Alemdar

Signature:

ABSTRACT

FUNCTIONALIZATION OF NANOMATERIAL: APPLIED FOR ENVIRONMENTAL REMEDIATION

Alemdar, Eda

M. Sc., Department of Chemistry

Supervisor: Prof. Dr. Semra Tuncel

Co-advisor: Prof. Dr. Gülsün Gökağaç

September 2017, 69 pages

Environmental pollution is a problem which is threatening living organisms and ecosystem with increasing rate every day. For decades, many studies have been done and experiments have been conducted in order to cure this serious danger. Organic pollutants in general is a big danger especially a group called Persistent Organic Pollutants (POPs) which are mostly originates from industrial and other man made sources are great danger. Among POPs, Polycyclic Aromatic Hydrocarbons (PAHs) are the most common ones. Therefore removal of PAHs from natural environment is a great concern. This study focuses on the synthesis and use of three nanocomposites which are 25% Fe_3O_4/MWCNT, 40% Fe_3O_4/MWCNT and 50%Fe_3O_4 /MWCNT, and then compare the synthesized materials PAH's removal efficiency with MWCNT and f-MWCNT. Materials used for removal or remediation are varied. Among them Carbon nanotubes (CNTs) are the cheapest and commonly used one. To make them target oriented remediation material, surface activation is performed. Synthesized Fe_3O_4 nanocomposites were characterized by Transmission Electron Microscopy (TEM), Fourier-Transform Infrared Spectroscopy (FTIR), Vibrating Sample Magnetometer (VSM) and X-Ray Diffraction (XRD) instruments and it was clearly understood that Fe_3O_4/MWCNT nanocomposites were synthesized successfully. To revelation to the adsorption feature, Gas Chromatography-Mass Spectrometry (GC-MS) was used. . For the GC-MS calibration, naphthalene, acenapthalene, acenapthyne, fluorene, phenantherene and anthracene r^2 values are 0,999, 0,998, 0,997, 0,999, 0,999 and 0,998, respectively. According to the results obtained, 40 mg of material was able to adsorb ∑6 PAH with an efficiency of 98% from the solution containing 0.1 ppm

PAH in 50 minutes. It has been observed that the purification of the synthesized materials can be easily carried out with the aid of a magnet after adsorption process, because of their great magnetic property.

Keywords: PAH, magnetite, MWCNT, GC-MS, adsorption

ÖZ

NANOMATERYALLERİN FONKSİYONLAŞTIRILMASI VE ÇEVRESEL İYİLEŞTİRMEDE KULLANIMI

Alemdar, Eda
Yüksek Lisans, Kimya Bölümü
Danışman: Prof. Dr. Semra Tuncel
Eylül 2017, 69 sayfa

Çevre kirliliği canlıları ve ekosistemi her geçen gün artan bir hızla tehdit eden bir problemdir. Bu ciddi tehlikeyi ortadan kaldırmak için yıllardır birçok çalışma ve deney yapılmaktadır. Organik kirleticiler genel olarak büyük bir tehlike iken, özellikle Kalıcı Organik kirleticiler denen, endüstri ve insan yapımı kaynaklardan gelen kirleticiler de büyük tehlike arz etmektedir. Kalıcı organik kirleticiler arasında polisiklik aromatik hidrokarbonlar (PAH) en yaygın olanlardır. Bu sebeple, bu kirleticilerin doğal çevreden uzaklaştırılması önemlidir. Bu çalışma, üç farklı nano kompozit (%25 Fe_3O_4/MWCNT, %40 Fe_3O_4/MWCNT ve %50 Fe_3O_4 MWCNT) sentezi ve kullanımına yoğunlaşmış, sentezlenen malzemelerin polisiklik aromatik hidrokarbonları uzaklaştırma verimi karşılaştırılmıştır. Uzaklaştırma ve iyileştirme için kullanılan malzemeler çeşitlilik göstermektedir. Bu malzemeler arasında Karbon nanotüp en ucuz ve en yaygın olanıdır. Karbon nanotüpü hedef odaklı iyileştirme malzemesi yapmak için yüzey aktifleştirme işlemi gerçekleştirilmiştir. Sentezlenen Fe_3O_4 nanokompozit transmisyon electron mikroskobu (TEM), fourier transform kızılötesi spektrometresi (FTIR), titreşimli numune manyetometresi (VSM) ve X-ışınları Kırınımı (XRD) cihazları ile karakterize edilmiştir ve Fe_3O_4/MWCNT nanokompozitin başarılı bir şekilde sentezlendiği açıkça anlaşılmıştır. Adsorpsiyon rolünü kanıtlamak için gaz kromatografisi-kütle spektrometresi (GC-MS) kullanılmıştır. Naftalin, acenapthalene, acenapthyne, fluorene,phenantherene ve anthracene maddelerinin GC-MS kalibrasyonu için r^2 değerleri sırasıyla 0,999, 0,998, 0,997, 0,999, 0,999 and 0,998'dir. Elde edilen sonuçlara göre, 40 mg malzeme 50

dakikada 0.1 ppm PAH solüsyonunda %98 verim ile adsorpsiyon yapabilmektedir. Sentezlenen malzemenin saflaştırılması, malzemenin manyetik özelliği sayesinde adsorpsiyon sonrasında mıknatıs ile kolayca yapılabilmektedir.

To my great family...

ACKNOWLEDGMENT

I owe my deepest gratitude to Prof. Dr. Semra Tuncel for her guidance, patience and support.

I would like to thank to Prof. Dr. Gülsün Gökağaç for her support during the modification of carbon nanotube studies, and I am very grateful for her guidance thorough every stage of research.

I would like to thank Prof. Dr. Ayşen Yılmaz and her research group for X-Ray Diffraction analysis.

I am truly grateful to my dear friends Pelin Akman and Elif Serel Yılmaz for their endless support and friendship, for being with me whenever I needed.

I would also like to thank my darling, Umut, for reminding me what butterflies feel like.

Last but not least, my most heartfelt appreciation goes to my family. I would like to thank them for their constant support in the pursuit of my dreams and more importantly, for always believing in me.

TABLE OF CONTENTS

ABSTRACT v

ÖZ vii

ACKNOWLEDGMENT x

TABLE OF CONTENTS xi

LIST OF FIGURES xiii

LIST OF TABLES xv

LIST OF ABBREVIATIONS xvi

CHAPTERS

1. INTRODUCTION 1

1.1 Importance of Persistent Organic Pollutants in the Environment 1

1.2 Remediation of Persistent Organic Pollutants (POPs) 7

1.2.1 Carbon Nanotubes as a Remediation Material 7

1.2.2 Treatment of the Surface of Carbon Nanotubes 8

1.3 Literature Survey 8

2. EXPERIMENTAL 15

2.1 Reagents and Materials 15

2.2 Synthesis of Fe_3O_4/MWCNT 15

2.3 Experimental Methods 17

2.4 Instruments and Apparatus 18

2.4.1 Gas Chromotography- Mass Spectroscopy(GC-MS) 18

2.4.2 Fourier-transform Infrared Spectroscopy (FT-IR) 20

2.4.3 X-ray Diffraction Analysis (XRD) 21

2.4.4 Vibrating Sample Magnetometer (VSM) 22

2.4.5 Transmission Electron Microscopy (TEM) 23

3. RESULTS AND DISCUSSION 25
3.1 Characterization of Fe_3O_4/MWCNT nanocomposites 25
3.1.1 Fourier-transform Infrared Spectroscopy (FT-IR) 25
3.1.2 X-ray Diffraction Analysis (XRD) 26
3.1.3 Transmission Electron Microscopy (TEM). 28
3.1.4 Vibrating Sample Magnetometer (VSM) 31
3.2 Optimization of Extraction Capacity of Nanocomposites 32
3.3 Optimization of Extraction Capacity 42
3.3.1 Effect of Dosage 42
3.3.2 Effect of Contact Time 43
3.4 Adsorption of PAHs by Different Nanocomposites 44
3.5 Adsorption Isotherms 48
3.6 Magnetic Property of Fe3O4/MWCNT Nanoparticles 51
4. CONCLUSION 55
REFERENCES 57
APPENDIX 63

LIST OF FIGURES

Figures

Figure 1. Molecular Structures of PAHs. 2
Figure 2. Incomplete Combustion Scheme of PAHs 3
Figure 3. Formation of PAHs by Pyrolysis 4
Figure 4. The Formation-Degradation Balance of PAHs 5
Figure 5. Adsorption of PAHs on CNT 7
Figure 6. Π –Π Interaction Between Naphthalene and CNT 8
Figure 7: Experimental Setup for the Synthesis Of Fe_3O_4/MWCNT 16
Figure 8. Molecular Structures of (a) MWCNT, (b) F-MWCNT and (c) Fe_3O_4/MWCNT 18
Figure 9. (a) 7mm Diameter Column, (b) Experimental Setup During Treatment of Pahs To The Nanoparticles 18
Figure 10. Experimental Setup for the Synthesis of Fe_3O_4/MWCNT 19
Figure 11. Block Diagram of the FTIR Spectroscopy 21
Figure 12. Block Diagram of XRD 22
Figure 13. Block Diagram of VSM 23
Figure 14: Schematic Representation of Working Principles of TEM 24
Figure 15: FT-IR Measurements of Fe_3O_4/MWCNT And f-MWCNT Composites 26
Figure 16. X-Ray Diffraction Patterns of 25% Fe_3O_4/MWCNT, 40% Fe_3O_4 /MWCNT and 50% Fe_3O_4/MWCNTS. 27
Figure 17. TEM Images of a) 25%, b) 40% and c)50% Fe_3O_4/MWCNT 29
Figure 18. Fe_3O_4 Nanoparticle on The MWCNT 30
Figure 19: The Magnetization Hysteresis Loops of Fe_3O_4/MWCNT Nanoparticles. 32
Figure 20: Calibration Curves of Nap, Acy And Ace 34
Figure 21: Calibration Curves for Flu, Anth And Phe 34
Figure 22: Scan Mode Spectrum of PAH Standard 36
Figure 23: Mass Spectrum for Naphthalene 37
Figure 24: Mass Spectrum for Acenaphtylene 38

Figure 28: Effect of MWCNT Dosage Mass on the Removal Percentage 43
Figure 29: Effect of Contact Time on the Removal Efficiency 44
Figure 30: First 10 Minutes into the Adsorption Process 45
Figure 31. Removal Efficiencies of Naphthalene on Different Adsorbents 46
Figure 32. Removal Efficiencies of Anthracene on Different Adsorbents 46
Figure 33. Removal Efficiencies of Fluorene on Different Adsorbents 47
Figure 34. Removal Efficiencies of Phenanthrene on Different Adsorbents..... 47
Figure 35. lnq vs. lnc Graph for the (A) Naphthalene, (B) Acenapthene, ... 50
(C) Acenapthylene, (D) Fluorene, (E) Phenanthenere And (F) Anhtracene……..50
Figure 36: Recovering of Fe_3O_4/MWCNTS from the Solution 53
Figure 37: Sım Mode Analysis of 0.5 Ppm Pah..... 64
Figure 38: 0.5 Ppm PAH After Adsorption by 40% Fe_3O_4/MWCNT In 5 Minute ... 65
Figure 39: 0.5 PpmPAH After Adsorption by 40%Fe3O4/MWCNT after 24 hours..66
Figure 40: Library Search Results from The GC-MS..... 69

LIST OF TABLES

Tables

Table 1. Maximum Permissible Concentrations (MPCs) by Agency For Toxic Substances And Disease Registry (ATSDR) 6
Table 2. Preparation of Fe_3O_4/MWCNT Nanoparticles 16
Table 3: Used Method for Gas Chromatography 20
Table 4. Values Set on the Mass Detector 20
Table 5. The saturation magnetization, coercivity and the remnant magnetization values for synthesized adsorbents 31
Table 6: Retention Times and Target Ion Numbers Obtained from Scan Mode Run 33
Table 7: LOD and LOQ Values of Studied PAHS 35
Table 8. Freundlich Constants For 6 PAHS 51

LIST OF ABBREVIATIONS

Ace -Acenapthylene

Acy -Acenaphtene

Ant –Anthracene

ATSDR - Agency for Toxic Substances and Disease Registry

BET -Brunauer–Emmett–Teller

CNTs -Carbon nanotubes

EMS -Eastern Mediterranean Sea

EPA -Environmental Protection Agency

Fe_3O_4- Magnetite

$FeCl_3.6H_2O$, Hydrated Iron(III) Chloride

$FeSO_4.7H_2O$, Hydreated Iron (II) Sulfate

Fle -Fluorene

f-MWCNT- Functional Multi Walled Carbon Nanotubes

FTIR- Fourier-Transform Infrared Spectroscopy

GC-MS-Gas Chromotography-Mass Spectrometry

H_2SO_4 – Sulfuric Acid

HNO_3- Nitric Acid

KBR: Potassium bromide

LOD : Limit of detection

LOQ: Limit of quantification

MDIS -Mechanically dewatered industrially sludge

MWCNTs- Multiwalled Carbon Nanotubes

Nap- Naphthalene

NH_4OH, Ammonium Hydroxide

OCPs -Organochlorine pesticides

PAHs-Polycyclic Aromatic Hydrocarbons

PCBs -Polychlorinated biphenyls

PDDA -Poly Dimethyl Diallyl Ammonium Chloride,

Phe -Phenantherene

POPs -Persistent organic pollutants

Ppb- Parts per billion

Ppm- Parts per million

TEM -Transmission Electron Microscopy,

TFs -Thin films

UNEP -The United Nations Environment Programme

VSM- Vibrating Sample Magnetometer

WHO-World Health Organization

XRD- X-Ray Diffraction

CHAPTER 1

INTRODUCTION

Thousands have lived without love, not one without water.
—Source: W.H. Auden: Collected Poems: Auden by W.H. Auden, 1991.

1.1 Importance of Persistent Organic Pollutants in the Environment

Persistent organic pollutants (POPs) are carbon based toxic chemicals; they can resist to environmental degradation and they can be widely distributed via soil, air and water[1]. Due to their endocrine disrupting feature, POPs affect health adversely, the World Health Organization (WHO) and the United Nations Environment Programme (UNEP) have arranged some regulations about their health and environmental impact. Among persistent organic pollutants, organochlorine pesticides (OCPs), polycyclic aromatic hydrocarbons (PAHs) and polychlorinated biphenyls (PCBs) are the ones which have high toxicity. 16 PAH prioritized by EPA and WHO are listed in the Figure 1.

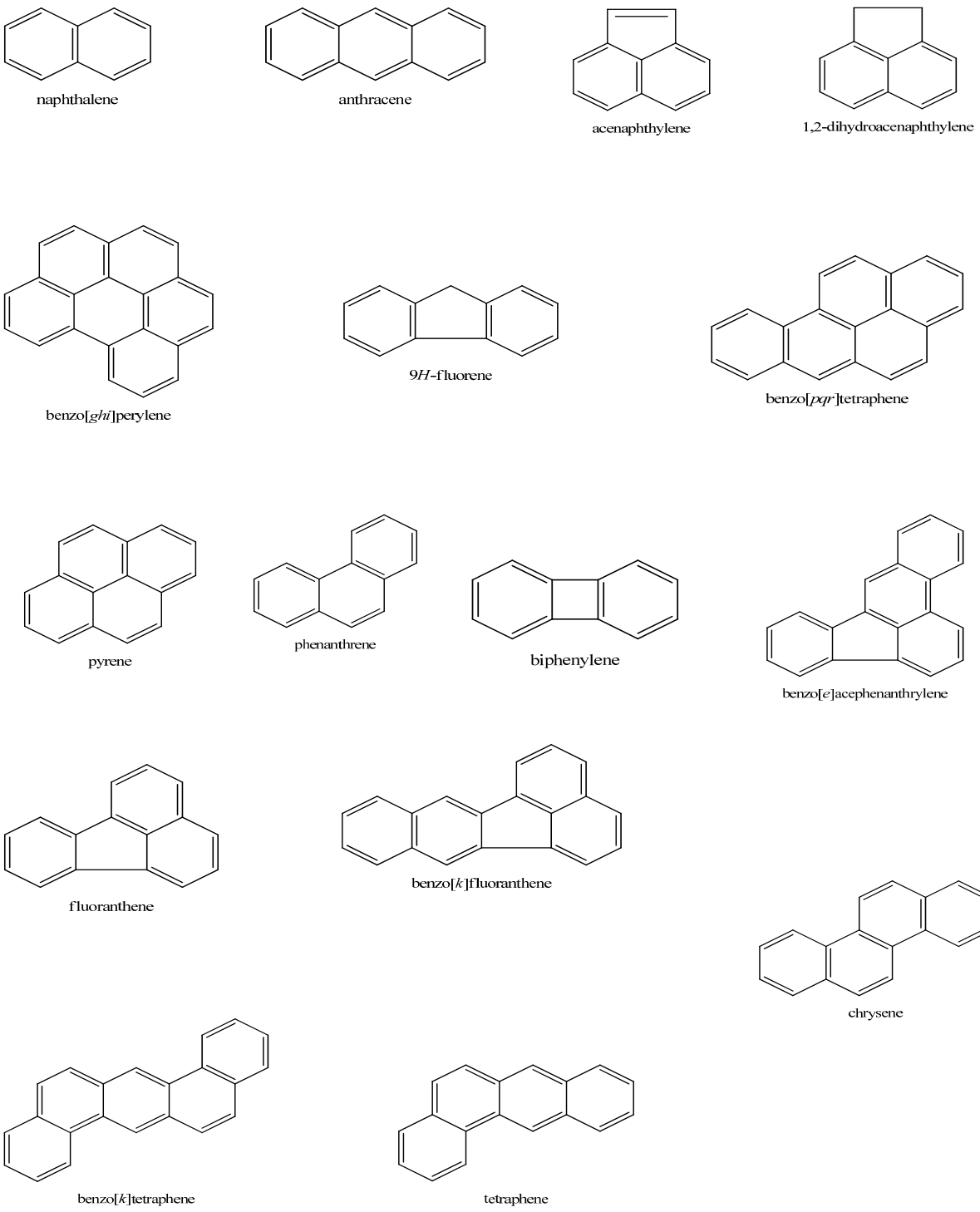

Figure 1. Molecular structures of PAHs.

These chemicals are originated from not only anthropogenic processes, i.e. incomplete combustion of organic materials, but also from natural events. The most common

characteristics for this class are; having high boiling and melting points, low water solubilities and low vapor pressures.

The formation scheme of the PAHs from the incomplete combustion is as in the Figure 2.

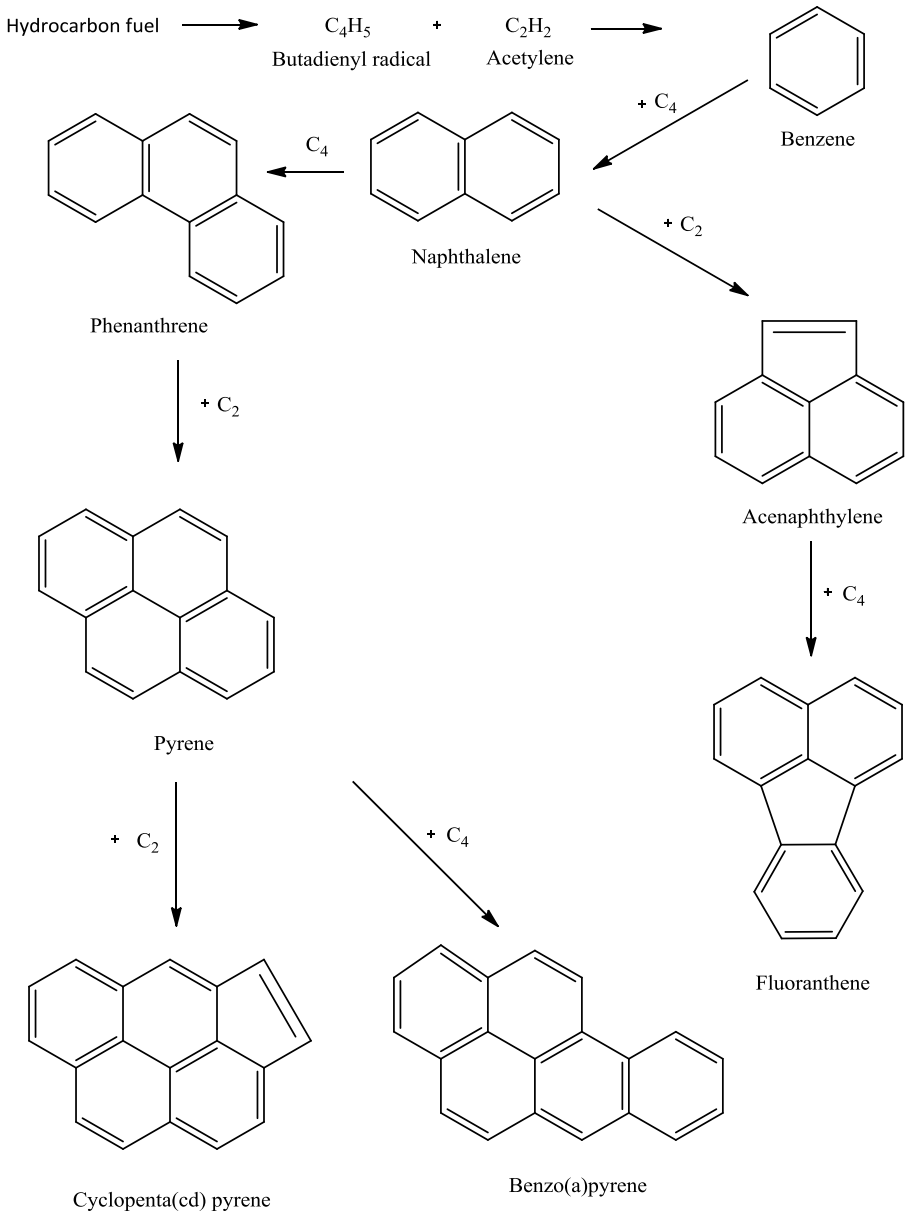

Figure 2. Incomplete combustion scheme of PAHs [2]

Another way of the formation of PAH is the pyrolysis and the formation reaction is given Figure 3.

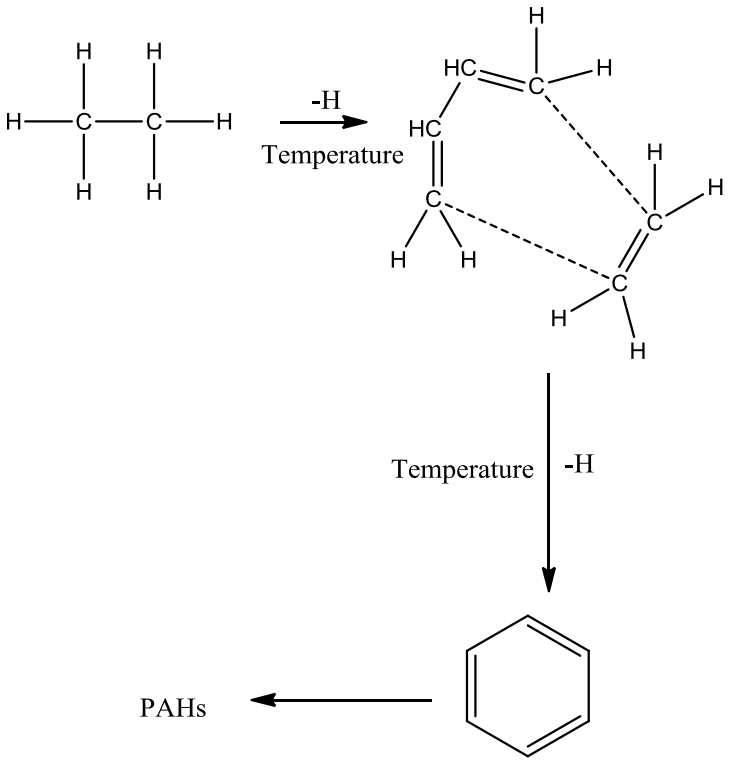

Figure 3. Formation of PAHs by pyrolysis

The way of releasing of PAHs into the air, water and soil are domestic burning, industrial processes and use of some household products. They cannot be removed from the environment in the short term. PAHs occur in nature due to natural causes such as volcanic explosions, pyrolytic reactions and open burning, and are resolved by photo fragmentation and biological transformations. There is a formation-degradation PAH balance between water, air and soil concentrations. Increasing industrial activities and used fossil fuels increase PAH emissions and disrupt this natural balance between the formation and degradation of PAHs. (Fig. 4). The global action of PAHs can be described as follows: PAHs, which are usually in the gaseous phase when they are first removed from the weld, are adsorbed on the particles during cooling and condensation. Particles can be transported with short and long ranges depending on their size and meteorological conditions. PAHs in gas and particulate phases suspended in air may precipitate by wet deposition (rain, adhesion on snow surface) and dry sedimentation (with effect of gravity) on land and water surfaces. Waves can be transported by winds to distances in the wind direction.

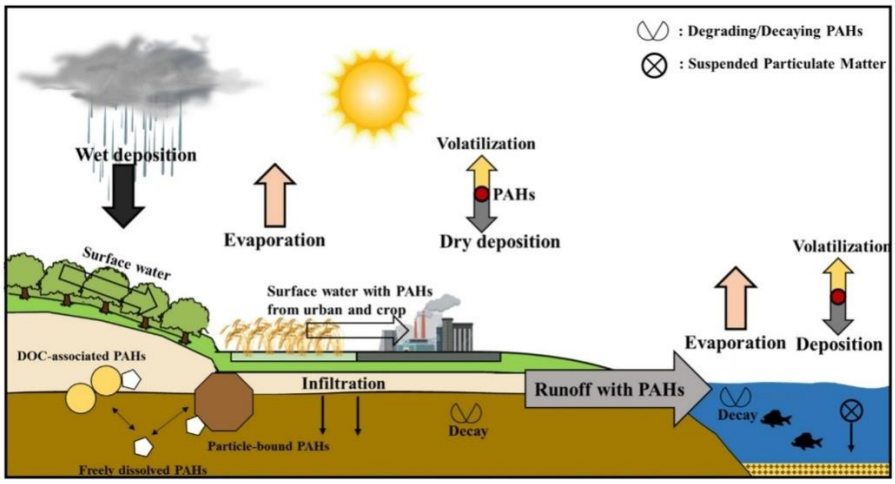

Figure 4. The formation-degradation balance of PAHs

They have a low degree of toxicity to humans but some studies have shown non-carcinogenic effects which depends on their exposure dose, problems on pulmonary, gastrointestinal, renal, dermatologic systems and diabetes and cancer are suggested as a POPs-related disease ([3], [4], [5]; [6]; [7]).

The chronic or long-term health effects of PAHs

The results of chronic and long-term exposure to PAHs on health are cataracts, kidney and liver damages and jaundices. Redness and skin inflammation may be the result of repeated exposure. If inhaled or ingested a lot red blood cells can breakdown. Laboratory studies show that when animals exposed to different levels of some PAHs for long periods of time resulting stomach cancer from eating of PAHs in food ,skin cancer from harming and lung cancer from breathing. It is indicated from the long-term studies showed that when workers are exposed to mixtures of PAHs and other workplace chemicals, they have a tendency to have lung, skin, bladder and gastrointestinal cancers.

At the same time, asthma like symptoms, lung function abnormalities and weakened immune function are identified in these studies. For all that the recorded usage of POPs has been withdrawn for many years by several countries; they persist at considerable levels in the nature in different environmental compartments worldwide. As a result of this persistence, most people are exposed to PAHs via air, water, soil and food sources regularly. As it was mentioned above, there is a balance between air, water

and soil, therefore PAHs concentration in these mediums are changing. However, some important events which affect the PAHs concentrations occurred throughout history. Industrial revolution is one of the example which causes sudden concentration change of PAHs. After industrial revolution, PAHs concentration increased dramatically, air pollution problems emerged and therefore living creatures faced health problems. Because of these problems first priority pollutants which causing health problem were determined by authority and then maximum allowable concentrations were set.

The maximum permissible concentrations (MPCs) of PAHs in soil and water [8] are presented in Table 1. No standards exist for the amount of PAHs allowed in the air, but it is recommended that the levels be no higher than 0.004 ppm. Although given limits were specified, measured PAH concentrations are generally higher than given concentrations, especially around industrial sites [9].

Table 1. Maximum permissible concentrations (MPCs) by Agency for Toxic Substances and Disease Registry (ATSDR)

PAH	MPC (Soil), ppm	MPC (Water), ppm
Naphthalene	1.0	3.0
Acenapththene	3.0	3.0
Acenaphthylene	3.0	3.0
Fluorene	3.0	3.0
Phenanthrene	3.0	3.0
Anthracene	3.0	3.0

1.2 Remediation of Persistent Organic Pollutants (POPs)

1.2.1 Carbon Nanotubes as a Remediation Material

Pollution has become a hot issue since from 1960's. Toxic chemicals which are include air, water and soil pollution causes to the environmental pollution. Biodiversity and degradation of human health are the results of this pollution. To minimize the health problems generating from the environmental pollution, using carbon based materials has increasing day-by-day. Carbon based nanomaterials have large surface area and they can adsorb not only organic pollutants but also metals on their surface. Among the carbon based nanomaterials, Carbon nanotubes (CNTs) have drawn attention because of their unique properties and potential applications. CNT adsorb organic pollutants on it because of hydrophobic interactions, π-π bonds, electrostatic interactions, and hydrogen bonds. Adsorption model is shown in Figure 5. The estimate the adsorption mechanism is not clear because adsorption efficiencies may change based on the pollutant's structure (polar or nonpolar) [10]. π -π interaction between PAHs and CNTs is represented in figure 6. Between CNTs and PAHs, mentioned interaction can also be occurred and in some studies pollutant water can be remediated with high yields by using CNTs [11].

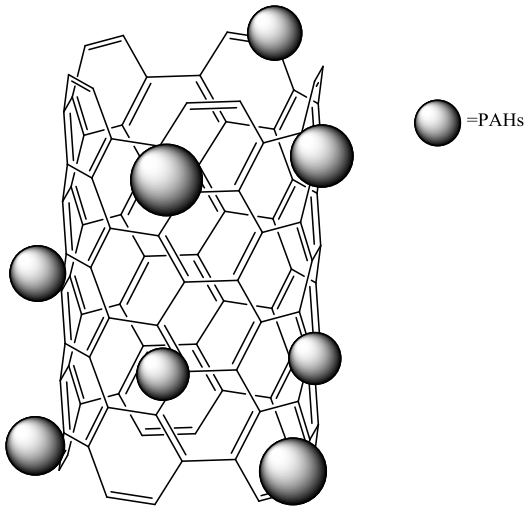

Figure 5. Adsorption of PAHs on CNT

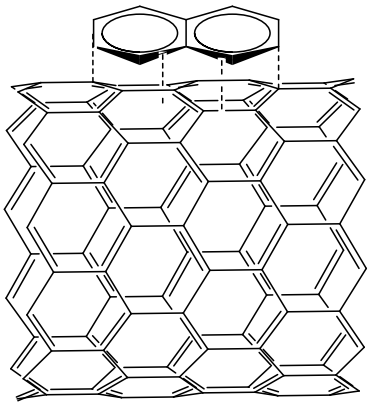

Figure 6. π –π interaction between naphthalene and CNTs

1.2.2 Treatment of the Surface of Carbon Nanotubes

It is known that CNT attracts PAHs and adsorb them on its large surface and finally air, water or soil can be cleaned from the pollutants. The aim treating on the surface of carbon nanotubes is to give the CNT additional features besides its adsorption capability; such as selectivity, magnetic property, etc.For this study, surface of CNTs will be treated and magnetic property was gained.

1.3 Literature Survey

This study focused on 6 PAHs (Figure 1) that the U.S. EPA has included in their priority list over hazardous substances in polluted waters. These 6 PAHs occur in highest concentrations and they have the largest risk of exposure. They are also regarded to be the most dangerous for the environment and health, and the damages they are causing are representative for the PAH

Due to the toxicity of PAHs, there are many studies on the removal of PAHs from the environment in the world. There are a number of studies in Turkey that have been carried out and continued. Our research group is one of the leading groups in the studies conducted for PAHs in our country. The first study, Eftade Gaga's doctoral dissertation, determined the levels, sources and distribution maps of PAHs in the environment by domestic heating in the Ankara atmosphere. As a result of this study,

the concentrations of PAHs in Ankara were inversely related to the socio-economic level and the concentration of the city was higher in the slum region. Eventually, fuel qualities of places where high concentrations are obtained are explained [12]. Moreover, another doctoral dissertation in our research group has also optimized the analytical methods for PAHs measurements in sediments by chemometric application [13].

In another study, to determine the atmospheric concentrations, distributions and air-soil exchange tendencies of PAHs in a heavily industrialized area in Kocaeli, 15 PAHs are analyzed in the soil samples at 23 sampling sites and the average PAH concentration were found as 285 ± 431 ng m^3 although the PAH limit [14].
Air and soil PAHs levels were investigated around coal-fired power plants and it was understood that power plants are the major sources for PAHs in Kütahya. Results were used for risk assessment and it was recognized that the percentage of the population exceeding the acceptable risk level ranged from <1% to 16%, except, 32% of the inhalation risk levels due to PAH exposure in winter in urban/industrial sites were $>10^{-6}$. While low molecular weight PAHs dominated the air pollution, higher molecular weight PAHs were founded in soil samples. At the end of the study, factor analysis applied to the data and showed that the major contributing PAH sources in the region were the coal combustion for power generation and residential heating (48.9%) and diesel and gasoline exhaust emissions (47.3%) [15].

PAH was measured in the gas and particulate phase over summer and winter sampling periods in Kocaeli, Turkey. Σ13PAH in the gas and particulate phases ranged from 6.2 ng/m^3 dibenz[a,h]anthracene to 98.6 ng/m^3 phenanthrene in the winter, and from 3.0 ng/m^3 benz[a]anthracene to 35.1 ng/m^3 phenanthrene in the summer. The most abundant PAH in both sampling periods was phenanthrene, followed by fluoranthene and pyrene. B[a]P toxic equivalency concentrations were found to be 3-fold higher in the winter months [16].

Some studies indicate that majority of priority PAHs was present in all sediment samples. To make explicit this argument, several studies have been carried out in Turkey to determine the PAHs in the coastal zone. One of them has been carried out in Izmit. Total PAH was measured in sea water, sediment and the mussel and the

resulting PAH concentrations are quite high. Average of the 16 PAHs in that region is in the range 1.16–13.68 mg/l in sea water, in the range of 30.0–1670.0 mg/g dry weight in sediments and in the range from 5.67 to 14.81 mg/g wet weight in edible part of mussel [17].

A total of 12 PAH measurements were made in Bursa in the work of Birgül and Tasdemir in 2015. While the total (gas + particulate) concentration of PAHs for the semi-rural sampling area was Σ12PAH 27 ng/m^3, this value was determined as 130 ng/m^3 for the other foot of the study. 37% of the total PAH concentration is in particulate form. The highest concentration levels were detected during the winter months when warming activities increased. It has been found that low molecular weight PAHs such as phenanthrene, anthracene and fluorene have higher concentration values than high molecular weight PAHs [18].

In the study conducted last year at the Eastern Mediterranean Sea(EMS), the total determined PAH concentrations (total of 16 compounds) resulting from the spatial and vertical profiles of the suspended particle-related polycyclic aromatic hydrocarbons (PAHs) collected from nine stations corresponding to various water column depths (1008-4087) results ranged between 90.6 and 918 pg/L. With the data obtained, it is stated that the deep Eastern Mediterranean Sea (EMS) waters formed a dirty warehouse. It is stated that the PAHs worked were composed of the common contribution of both fossil and pyrolytic compounds. The aquatic duration of PAHs associated with suspended particles is calculated to be about 30 years (only considering particle sedimentation) [19].

Another study was conducted in Kutch Bay (Jamnagar road), Gujarat, India to investigate PAH exposure and the adverse effects caused by it. In the study conducted, it is stated that the concentration of 2-3 ring PAHs (79.09%) is quite high compared to the concentration of 4,5 and 6-ring PAHs (20,91%). Carcinogenic PAH concentrations can be distributed between 8120-160,000 ng g^{-1} with 63,810 ng g^{-1}dw, much higher than with normal acceptable values. It is revealed that the Gulf of Kutch bears a great risk and can be considered a historically contaminated site when compared to the existing data at other sites globally [20].

The most comprehensive study of PAHs in recent years has been published this year in the United States. In this study, daily monitoring of PAH from 1990 to 2014 was monitored at 169 monitoring stations. The aim of this study is to examine the long-term trends of PAHs and to calculate the cancer risk. The predominant PAH sources were from traffic and non-traffic related fuel combustions with a dominant contribution from diesel emissions. As a result of the study, the average cancer risk from 10 carcinogenic PAHs was calculated as $9.3 \pm 30.1 \times 10^{-6}$. Finally, it is proposed to focus on reducing PAH exposure by controlling diesel emission and extending the geographic coverage of air monitoring [21].

It is undeniable that PAHs in the world and in Turkey are a very dangerous and toxic material. New methods for removing PAHs from air, water and soil should be found and existing methods should be developed. Because carbon based nanomaterials are cheap and relatively durable.

One of CNT's industrial applications is the use of environmental remediation methods. Although this area of use is quite new, there is a great increase in researches on this subject in the world. This increase has hastened especially in the last 5 years. The most important reason is that the destruction of organic pollutants on environment-human health is becoming clearer over time. This situation has also increased the importance of environmental remediation.

The studies carried out in the world are in the experimental scale in the laboratory and there is no industrial use yet. There are many studies in the laboratory scale. For example, in Malaysia, MWCNTs are an effective and innovative method for absorbing organic, inorganic and biological pollutants [22]. In another study in Iran, it was reported that MWCNTs were also used to determine the phthalates in urea samples using the solid phase extraction method [23].

It has also been described in a research in China that the large amount of water contaminated with Polychlorinated biphenyls (PCBs), which are toxic pollutants from the POP family, was again cleaned with the carbon nanotube-based synthesized material, Fe_3O_4 Grafted Multiwalled Carbon Nanotubes with Poly Dimethyl Diallyl Ammonium Chloride, MWCNTs-COO−/PDDA@Fe_3O_4 [24].

There are also studies in Turkey in this area. For example, in another research conducted in Çorlu, mechanically dewatered industrially sludge (MDIS) was treated

with pure and silver doped thin films (TFs) on quartz substrates. Microwave extraction technique was used to extract both PAHs and PCB from soil and it was observed that titanium and silver nanocomposites have been used successfully to clean industrial zone soil samples containing PAH and PCB [25].

In recent years, researchers have been interested in the fact that surfaces of CNTs are activated and turned into target-oriented materials. In this context, different functional groups were attached to the surfaces of CNTs to try to gain selectivity for certain pollutants. The nature of CNTs is insoluble in many organic solvents and water. Surface activation and modification ensure that this material is compatible and selective.

Fe_3O_4-MWCNT nanoparticles have been used incrementally in electrochemical applications because of their incomparable magnetic and electrical properties, among the metal oxide nanoparticles. Due to many unique properties such as higher bioactivity, large surface area, excellent conformation stability and good contact between biocatalyst and its substrate, nano scale magnetic materials have been used in electrochemical biosensor devices. The large amount of pesticide residues is a threat to global health by inhibition of acetylcholinesterase (AChE) in the environment. The integration of MWCNTs and Fe_3O_4 nanoparticles is expected to provide a synergistic effect in construction of AChE biosenors. For instance, in a study, AChE onto Fe_3O_4/MWCNT modified gold electrode were developed with immobilizing covalently strategy and addressed its application in construction of an amperometric biosensor for determination of pesticides [26]. With this sensor pesticide determinations can be done with high biocompatibility, high sensitivity and good stability.

In another study, Fe_3O_4-MWCNT magnetic nanocomposites were used as an efficient peroxidase mimic catalyst for water purification. With this study, it was demonstrated that Fe_3O_4-MWCNT nanocomposites adsorb methylene blue (MB) dye and therefore removal of MB were resulted with nearly 100% of MB decolorization obtained under optimal experimental conditions. It was stated that because of the magnetic property

of Fe3O4/MWCNT nanocomposites, separation process was finished quickly by a magnet and degradation process was finished.

Aim of the Study

Main aim of this study was to synthesize Fe_3O_4/MWCNT nanocomposites with different Fe ratios and examine the adsorption behavior of PAHs on the synthesized magnetic nanocomposites. Besides this main purpose, we were also aimed:

- to make characterization studies with different instruments(FT-IR, TEM, XRD, BET, VSM)
- to make an adsorption behavior comparison with MWCNT and f-MWCNT because surface areas of these materials are different.
- to make optimisation of extraction process

CHAPTER 2

EXPERIMENTAL

2.1 Reagents and Materials

$FeCl_3.6H_2O$, NH_4OH, $FeSO_4.7H_2O$, H_2SO_4 and HNO_3 were the analytical grade. PAH standard solutions (PAH-Mix 68, 100.00 mg/L) was purchased from Dr. Ehrenstorfer Augsburg, Germany). MWCNT is purchased from Sigma Aldrich. Functional Multi walled carbon nanotube (f-MWCNT) was bought from Nanografi. In the Fe_3O_4-MWCNT synthesis process, 18 Mohm deionized waterwater was used for the all processes. Glass wool was purchased from Supelco.

2.2 Synthesis of Fe_3O_4/MWCNT

About 0.1 g f-MWCNT was dissolved in 60 mL of water and ultrasonicated until it completely dispersed. The mixture was further stirred vigorously for 30 min at 60 ^{0}C under nitrogen atmosphere in 4-port flask. Then 153 mg of $FeCl_3.6H_2O$ were run in under stirring and reacted 30 minutes finally 80 mg of $FeSO_4.7H_2O$ was added and again 30 min stirred. Finally 30 ml of 6% NH_4OH aqueous solution was added into the mixture at 60 ^{0}C during 1 hour and reaction continued. The whole process was performed under nitrogen atmosphere. To hold temperature constant, soil bath was used. Then the mixture was filtered and washed until it become pH=7. Experimental setup is shown in Figure 6. During the synthesis, following reaction occurs;

$$MWCNT + Fe^{2+} + 2Fe^{3+} + 8OH^- \longrightarrow Fe_3O_4/MWCNT + 4H_2O$$

25% Fe_3O_4/MWCNT, 40% Fe_3O_4/MWCNT and 50% Fe_3O_4/MWCNT were prepared according to the table below:

Table 2. Preparation of Fe_3O_4/MWCNT nanoparticles

	Fe_3O_4/MWCNT (mg)	MWCNT (mg)	Percentage (w/w)	$FeSO_4.7H_2O$ (mg)	$FeCl_3.6H_2O$ (mg)	NH_4OH (6%) (mL)
25% Fe_3O_4-MWCNT	33,0	100,0	50%	40,0	77,2	15,0
40% Fe_3O_4-MWCNT	66,0	100,0	40%	80,0	153,0	30,0
50% Fe_3O_4-MWCNT	99,0	100,0	25%	120,0	229,5	45,0

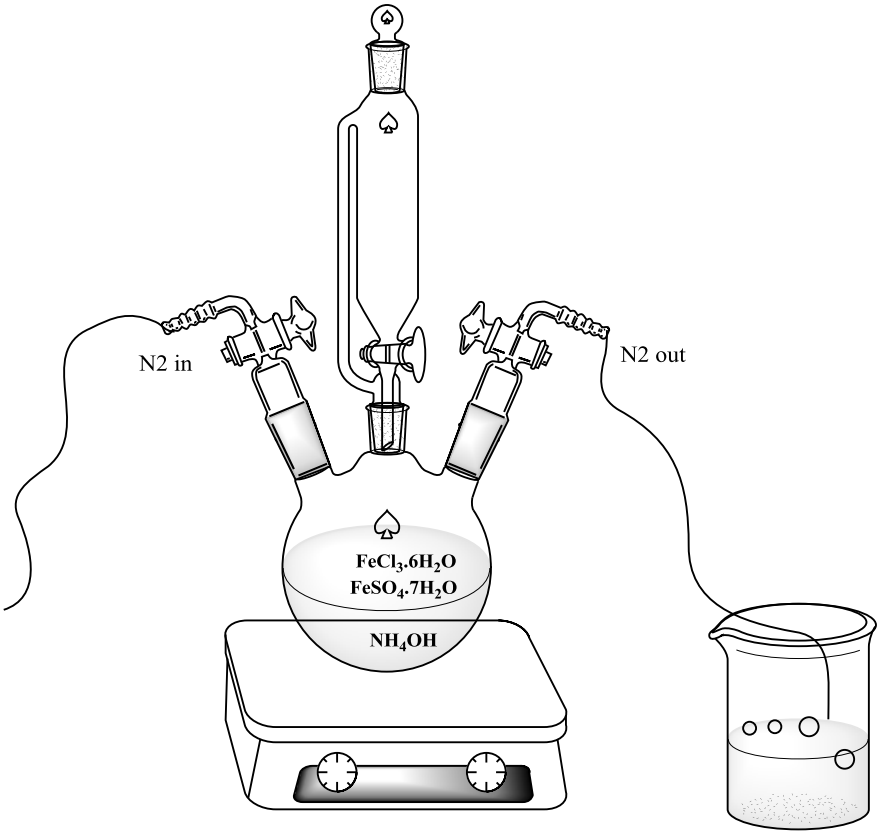

Figure 7: Experimental Setup for the synthesis of Fe_3O_4-MWCNT

2.3 Experimental Methods

For this study, 5 adsorbents were chosen for the remediation of PAHs from wastewater, which are MWCNT, f-MWCNT, 25% Fe_3O_4/ MWCNT, 40% Fe_3O_4/ MWCNT and 50% Fe_3O_4/ MWCNT. Although MWCNT has shown great adsorbent for PAHs, Fe_3O_4/ MWCNT nanoparticles were synthesized, because Fe_3O_4/ MWCNT nanoparticles are magnetic and they can be separated easily from the solution. f-MWCNT is a starting material for the Fe_3O_4/ MWCNT synthesis.

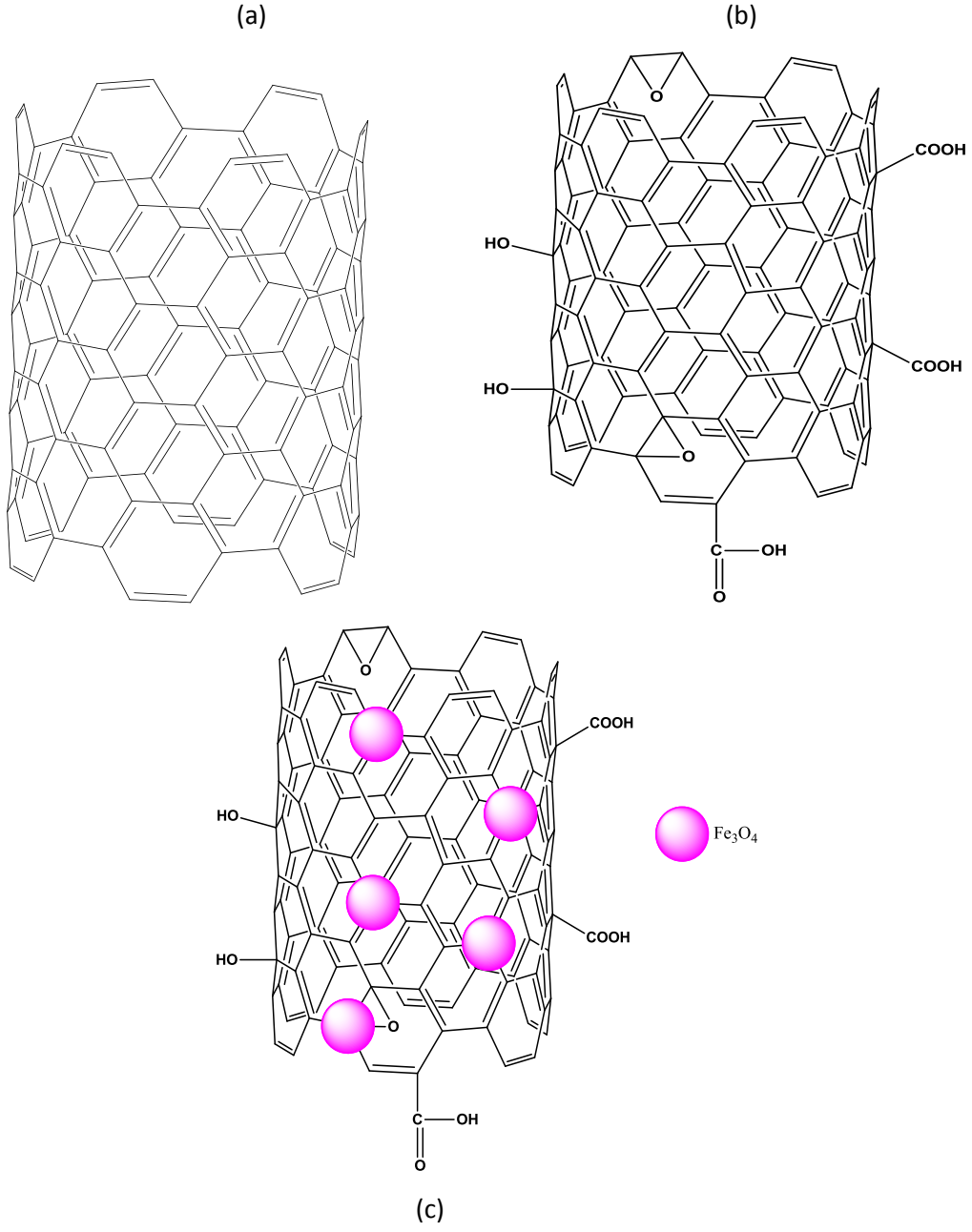

Figure 8. Molecular structures of (a) MWCNT, (b) f-MWCNT and (c) Fe3O4/MWCNT

The method for the treatment of PAH standard solution was developed in our research group. The tips of the custom made glass tubes (having a diameter of 7mm) (Figure 7) were filled with glass wool, then selected adsorbent was placed on top of the glass wool. The prepared sample solutions were slowly added dropwise and flowed through the adsorbent for the adsorption of the PAHs and the eluted solution can be ready for the GC-MS analysis.

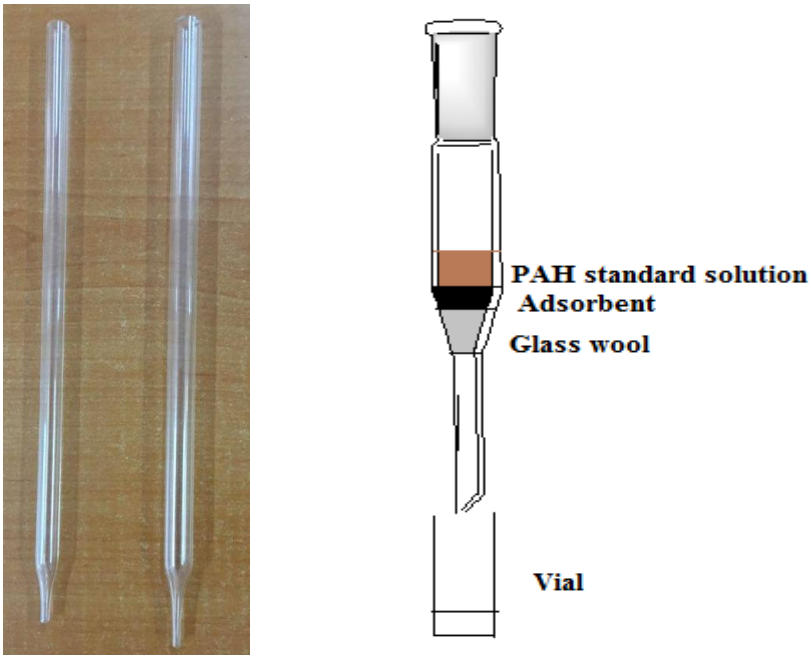

(a) (b)

Figure 9. (a) 7mm diameter column, (b) experimental setup during treatment of PAHs to the nanoparticles

2.4 Instruments and Apparatus

2.4.1 Gas Chromotography- Mass Spectroscopy(GC-MS)

To examine a wide range of compounds sensitively and selectively, chromatography technique is used. In chromatography, chemicals in the analytes can be separated as for that their polarities and volatilities. If the analyte's polarity is similar with the column, analyte stays in the column long time, on the other hand, analyte's polarity is unlike with the column, analyte's retention time will be less. Helium, hydrogen or nitrogen gases are often used as the eluent (mobile phase) in gas chromatography.

Retention time is the major information used to identify the compound. However, when two or more compounds have very close retention times identification and separation becomes very difficult. For this cases, using mass spectrometer is mandatory.

In the mass spectrometer, a molecule ionized and separated into their fragments, its ions and they have different masses. Using mass spectrometry near to the gas chromatography means that molecules have a fingerprint. Almost every molecule can be recognized with that instrument. In this technique, using vacuum system is important.

For the analysis, a HP (Hewlett Packard) 6890 series gas chromatograph with HP 5973 mass spectrometer was used. A 30m, 0.32 mm id., 0.25mm film thickness, cross-linked 5% Phenyl methyl siloxane, HP 5MS, capillary column was used for the separation of analtye throughout the study. Gas Chromatography-Mass Spectrometry was used for the determination of PAHs.

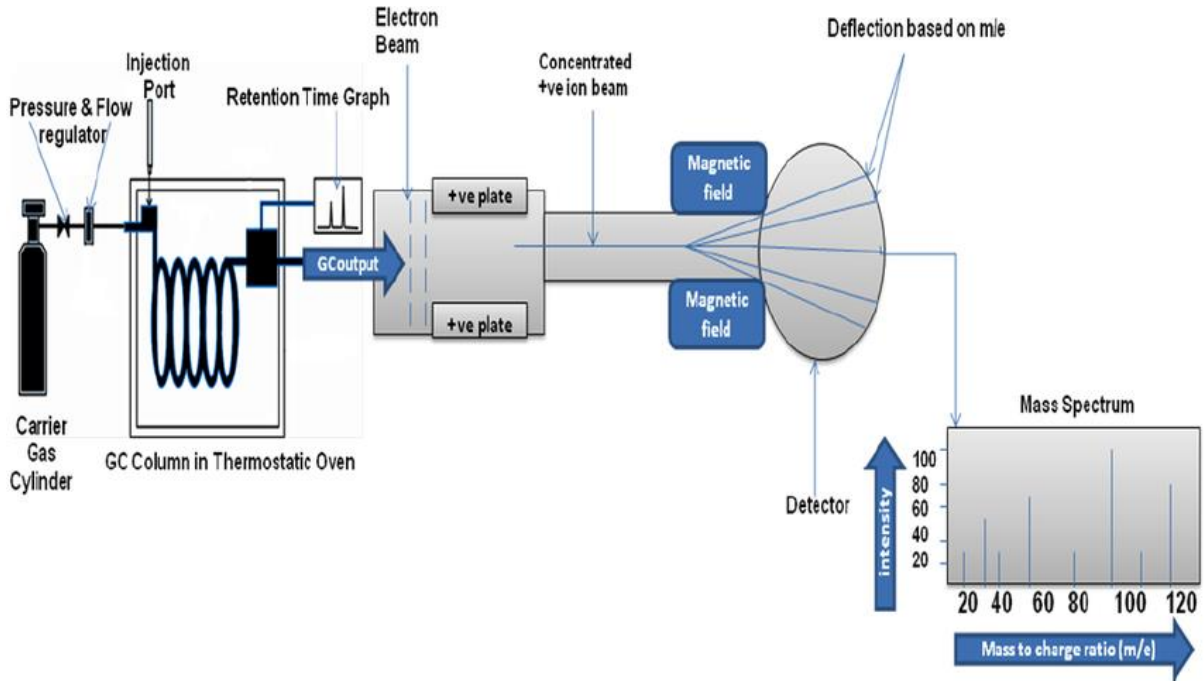

Figure 10. Experimental Setup for the synthesis of Fe3O4-MWCNT

The sample solutions were analyzed before and after the treatment with CNT to calculate the percentage of the PAHs that were adsorbed on the Fe_3O_4/MWCNT. Table 2 shows method of the instrument.

Table 3: Used method for Gas Chromatography

Injector:	Splitless
Inlet temperature:	295ºC
Column:	HP-5 MS (5 % Phenyl Methyl Siloxane 30.0m*0.25mm*0.25 mm)
Oven temperature:	80ºC-180ºC at 15º C/min. 5 mins. 150ºC-300ºC at 5 º C/min. wait for 2mins.
MS source temperature:	290ºC
MS quadrupole temperature:	150ºC
Injection volume:	2 µl
Carrier gas:	Ultra purified Helium, 99.99%. 1mL/min

Table 4. Values set on the Mass Detector

Item	**Condition**
Electron Energy	70 Volts (nominal)
Mass Range	35-300 amu
Scan Time	To give at least 10 scans per peak, not to exceed 1 second per scan

2.4.2 Fourier-transform Infrared Spectroscopy (FT-IR)

KBR pellets are used to measure background absorption. KBr and analyte pellets were prepared and analyzed with a Bruker 66 v/s instrument acquiring 32 scans per specimen at a nominal resolution of 4 cm^{-1}. In the origin, 7 points get together and smoothed. MWCNT, MWCNT-COOH and Fe_3O_4-MWCNT spectra were taken. Block diagram of the FTIR spectroscopy is shown Figure 11.

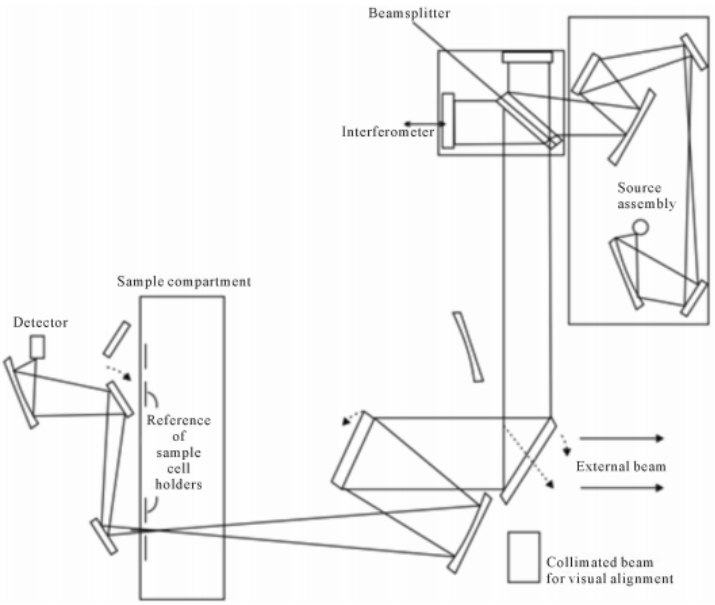

Figure 11. Block diagram of the FTIR spectroscopy[27]

2.4.3 X-ray Diffraction Analysis (XRD)

To get the crystal structure of the material, X-ray diffraction is one of the most confidential method. Cystal structure of Fe_3O_4/MWCNT was investigated by the powder XRD measurements. Rigaku Miniflex X-Ray Diffractometer instrument was used for the analysis with Cu-Kα at 30 kV and 15 mA source. (λ=1,5405 Å) . The range of 2θ degree was set between 10^o and 90^odegrees. Scanning speed was 1^0 per minute. Powder samples were used for XRD analyses. Figure 12 shows the working scheme of the XRD.

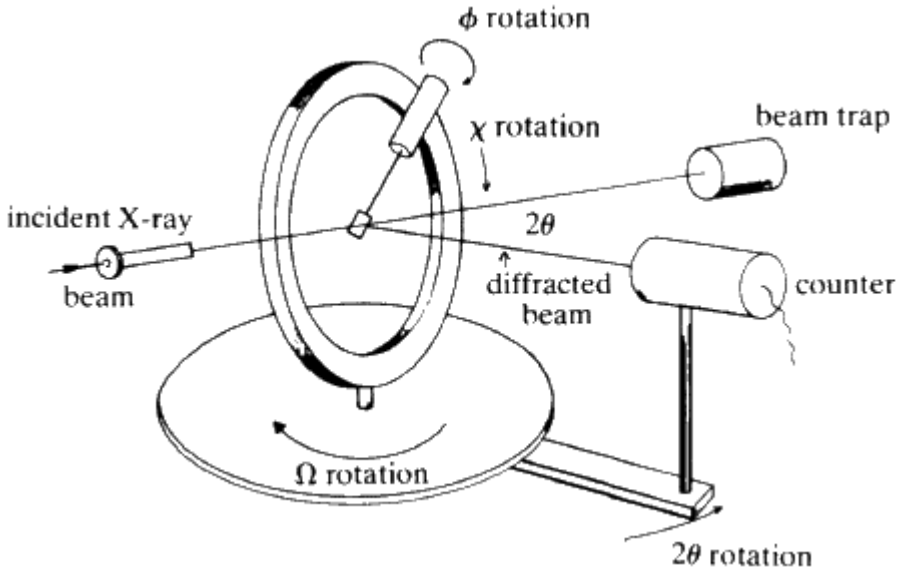

Figure 12. Block Diagram of XRD

2.4.4 Vibrating Sample Magnetometer (VSM)

Cryogenic Limited PPMS instrument was used to get information about magnetic properties of the sample. VSM analyses were done in METU Central Laboratory. Like XRD method, powdered samples were used for the analysis. Powdered samples were filled into small cylindrical containers made of acrylic glass, then they were weighed and recorded. Magnetization values obtained by applying a magnetic field of 20 kOe to the samples were measured at room temperature. The magnetizations of the particles in the magnetic field are expressed as the magnetic moment per unit mass (emu / g) [28]. Figure 13 represents to the block diagram of VSM.

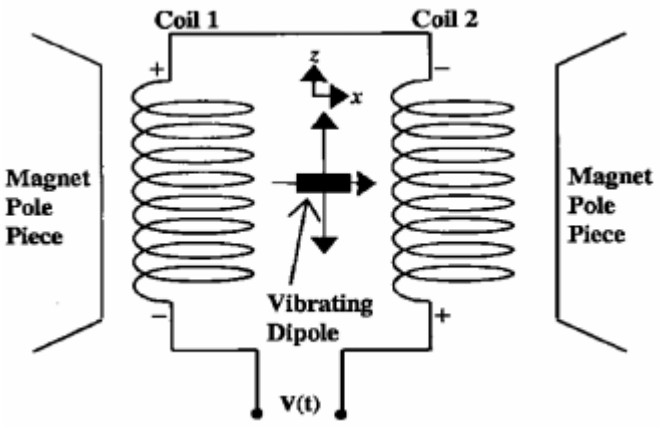

Figure 13. Block Diagram of VSM

2.4.5 Transmission Electron Microscopy (TEM)

Electron microscopy can be defined as a science field that uses an electron microscope as a tool and uses an electron beam to create an image of a sample. The electron microscope utilizes a very short wavelength of $\lambda = 0.05$ Å electron. Electrons interact with atomic particles of the samples and then images of the samples can be drawn. The samples can be enlarged from 500 to 500,000 of their original size, allowing them to be examined at the nanometer size [29].TEM technique projects electrons through an ultrathin slice of the sample and produces a two dimensional image. The electron source,the imaging system and the objective lens are the three compartments of TEM. Electron gun produces electrons with an energy in between 20 - 1000 keV, then they are sent on the sample with a desired diameter using electromagnetic lens. Several lenses are used to magnify the image and focuses them on the computer display via a detector. Figure 11 shows the block diagram of TEM instrument[30]. For this work, 25% Fe_3O_4/MWCNT, 40% Fe_3O_4/MWCNT and 50% Fe_3O_4/MWCNT nanocomposites were dissolved in 1, 5 mL ethanol and ultrasonicated until powder particles were dispersed. Then few drops were dropped on copper grid and left to dry in clean atmosphere. The slit was then taken as a tab and introduced to the instrument. TEM images of the samples were taken by JEOL 200 kV TEM instrument in Central Laboratory at METU.

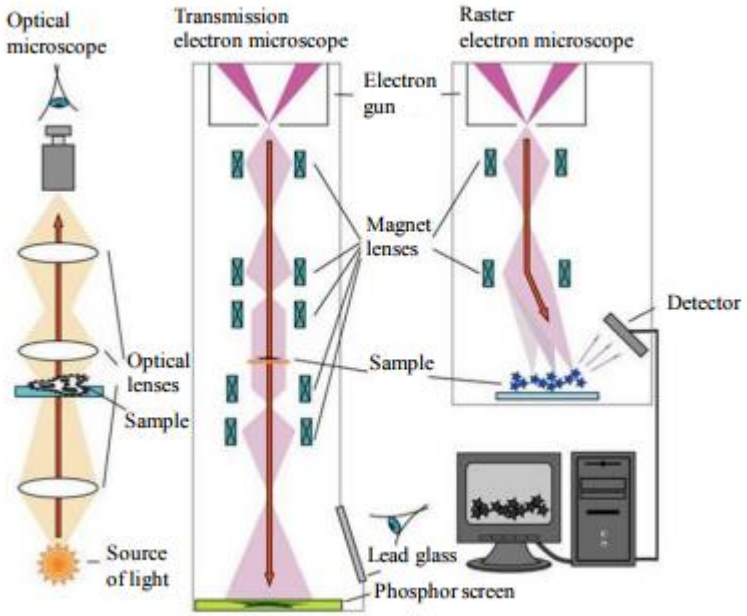

Figure 14: Schematic Representation of working principles of TEM

CHAPTER 3

RESULTS AND DISCUSSION

3.1 Characterization of Fe_3O_4/MWCNT nanocomposites

Characterization of nanocomposites were done by using Fourier-transform Infrared Spectroscopy (FT-IR) and X-Ray Diffraction Analysis (XRD) instruments available in our department, Transmission electron microscopy (TEM), Brunauer–Emmett–Teller (BET) and Vibrating Sample Magnetometer (VSM) instruments from METU Central Laboratory.

3.1.1 Fourier-Transform Infrared Spectroscopy (FT-IR)

Fourier-transform Infrared spectroscopy is a versatile instrument and concerned as the study of absorption of infrared radiation. When a molecule absorb the Infrared radiation, because of the energy, vibration transition is observed, that's why IR spectroscopy also known as Vibration spectroscopy. IR spectra mainly used to determine the functional groups.

The 40% Fe_3O_4-MWCNT nanocomposites were analyzed by FTIR spectroscopy throughout the range of 400–4000 cm^{-1} and result is presented in Figure 12 as a shifted spectra. It can be observed that the FTIR spectra of the Fe_3O_4/MWCNT contain bands at 586 cm^{-1} assigned to the Fe–O–Fe stretching and bending modes, which is an indication of the presence of Fe_3O_4 in the 40% (w/w) Fe_3O_4/ MWCNT. The band at 1558 cm-1 was the characteristic graphite structure peak, which was assigned to the C=C groups of the CNTs. In the f-MWCNT spectrum, which is bought commercially, adsorption peaks at 1500 and 1720 indicates the –COOH functional groups in the f-MWCNT.-OH vibration shows the relatively moderate peak located at 3436 cm^{-1}, indicating the presence of OH groups in the spinel lattice structure and probably on the surface of Fe_3O_4, which is derived from the absorbed H_2O. The undermost spectrum belongs to the Fe_3O_4-MWCNT and the uppermost spectrum belongs to the f-MWCNT.

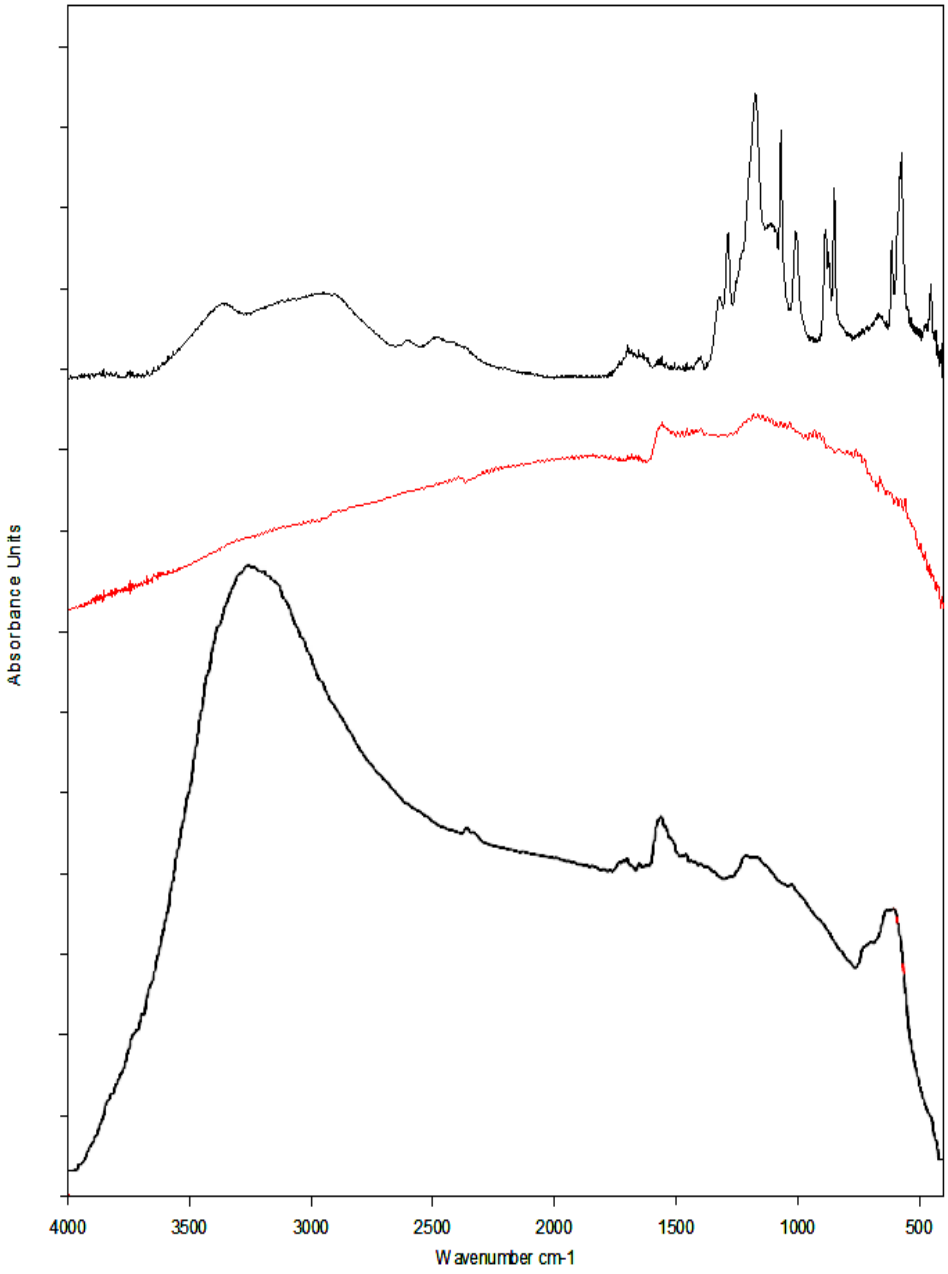

Figure 15: FT-IR measurements of Fe3O4-MWCNT and f-MWCNT composites

3.1.2 X-ray Diffraction Analysis (XRD)

This instrument provides information about the crystalline structure of nanocomposites.

The prepared 25%Fe_3O_4/MWCNT, 40% Fe_3O_4/MWCNT and 50% Fe_3O_4/MWCNT nanocomposites and commercially available MWCNT and f-MWCNT were examined by XRD characterization. The crystalline diffraction peaks at 30.35, 35.59, 43.33,

57.12 and 62.88 were identified as the (220), (311), (400), (511) and (440) planes of the spinel phase of Fe_3O_4, respectively. MWCNT's diffraction peak is at 26.4 and the ratio of (220) peak to the CNT peak increasing with increasing percentage of Fe_3O_4. The XRD results indicated that Fe_3O_4/MWCNT nanocomposites were successfully synthesized.No crystalline impurities were detected.

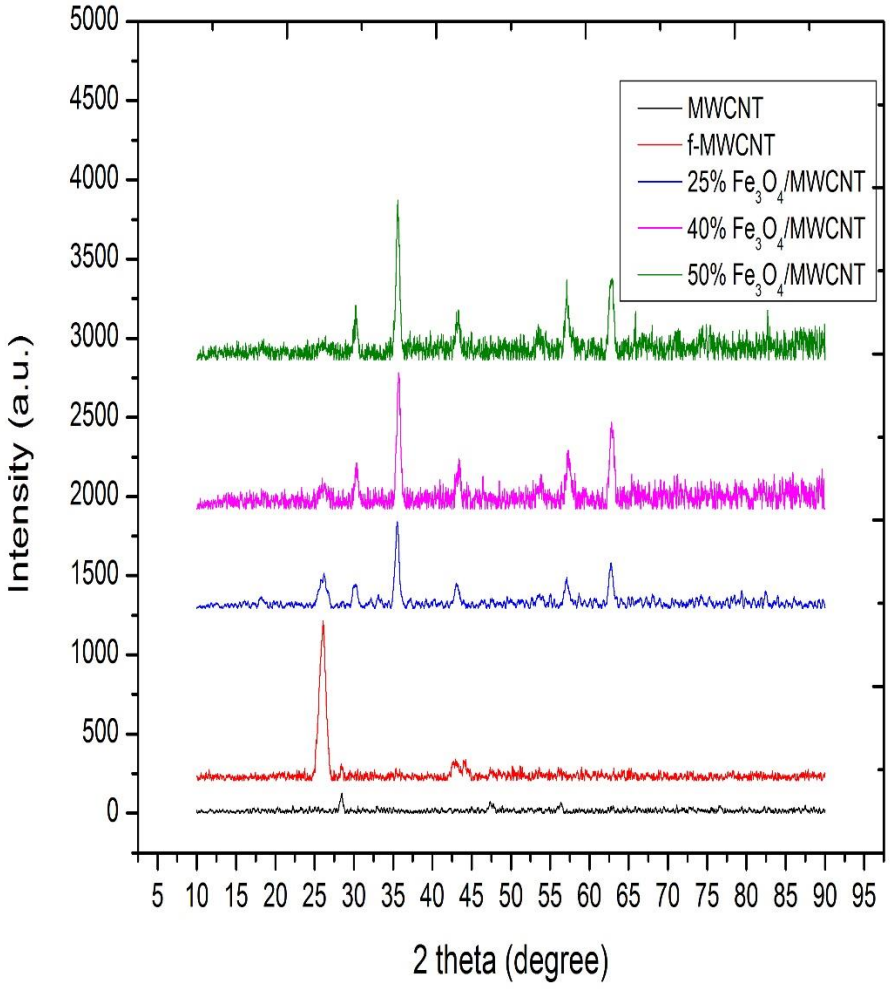

Figure 16. X-ray diffraction patterns of 25% Fe_3O_4-MWCNT, 40% Fe_3O_4 –MWCNT and 50% Fe_3O_4–MWCNTs.

3.1.3 Transmission Electron Microscopy (TEM).

TEM, as one of the most useful methods to characterize the morphologies of nanoparticles in nanocomposites, has been used for the investigation of the hybrid material. 200 nm views of three nanocomposites are given in Figure 14. TEM images reveal the coverage/ decoration of MWCNT with Fe_3O_4nanoparticles. It should be pointed out that Fe_3O_4 nanopa rticles are firmly anchored on the surface of MWNT because of their magnetic property. The strong combination of Fe_3O_4nanoparticles and MWCNT can be attributed to covalent interaction through the functional groups on the surface of the modified MWCNT. Average size of Fe_3O_4nanoparticles was estimated as 9nm. It can be clearly seen that, as the percentage of Fe_3O_4 increases, the agglomeration also increases. Figure 17a, 17b and 17c show the closer view to the Fe_3O_4 particles. Figure 18 shows the closer view of Fe_3O_4 particles.

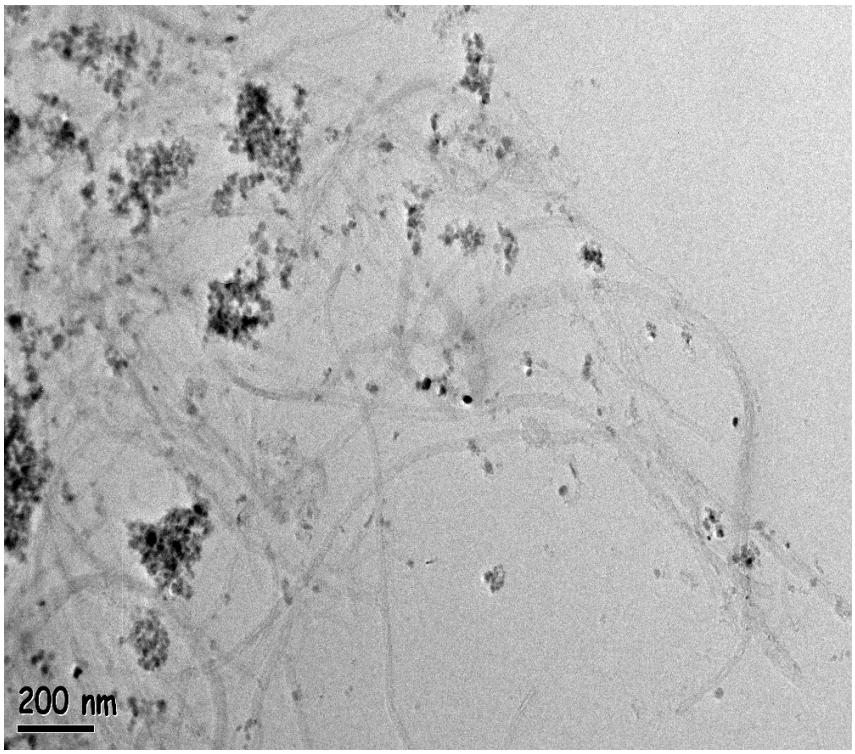

(a)

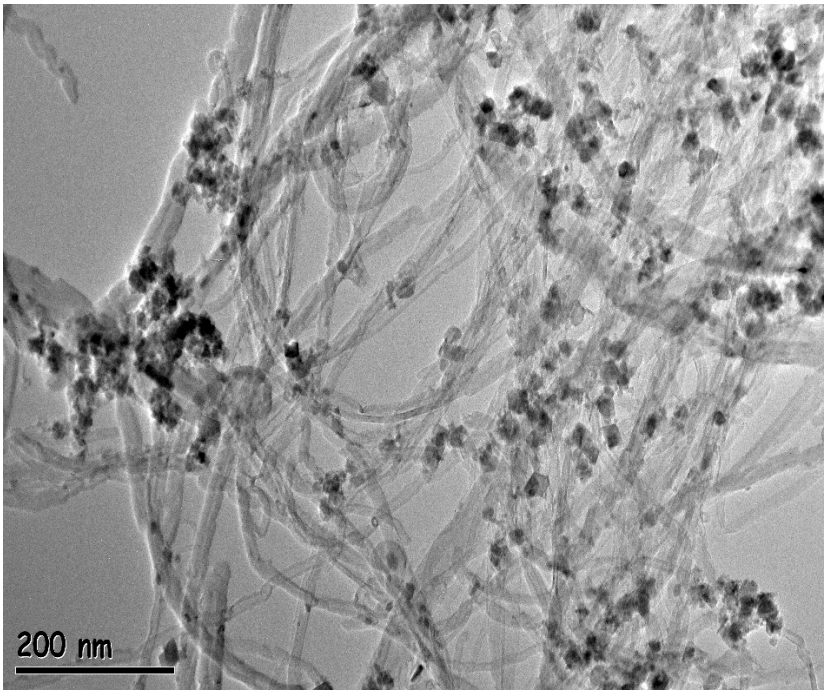

(b)

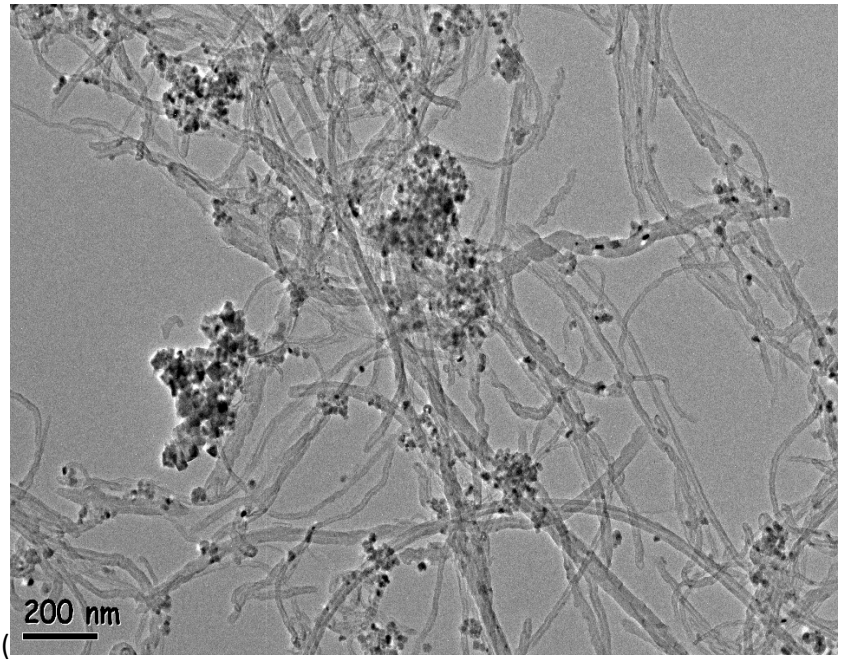

(c)

Figure 17. TEM images of a) 25%, b) 40% and c)50% Fe_3O_4/MWCNT

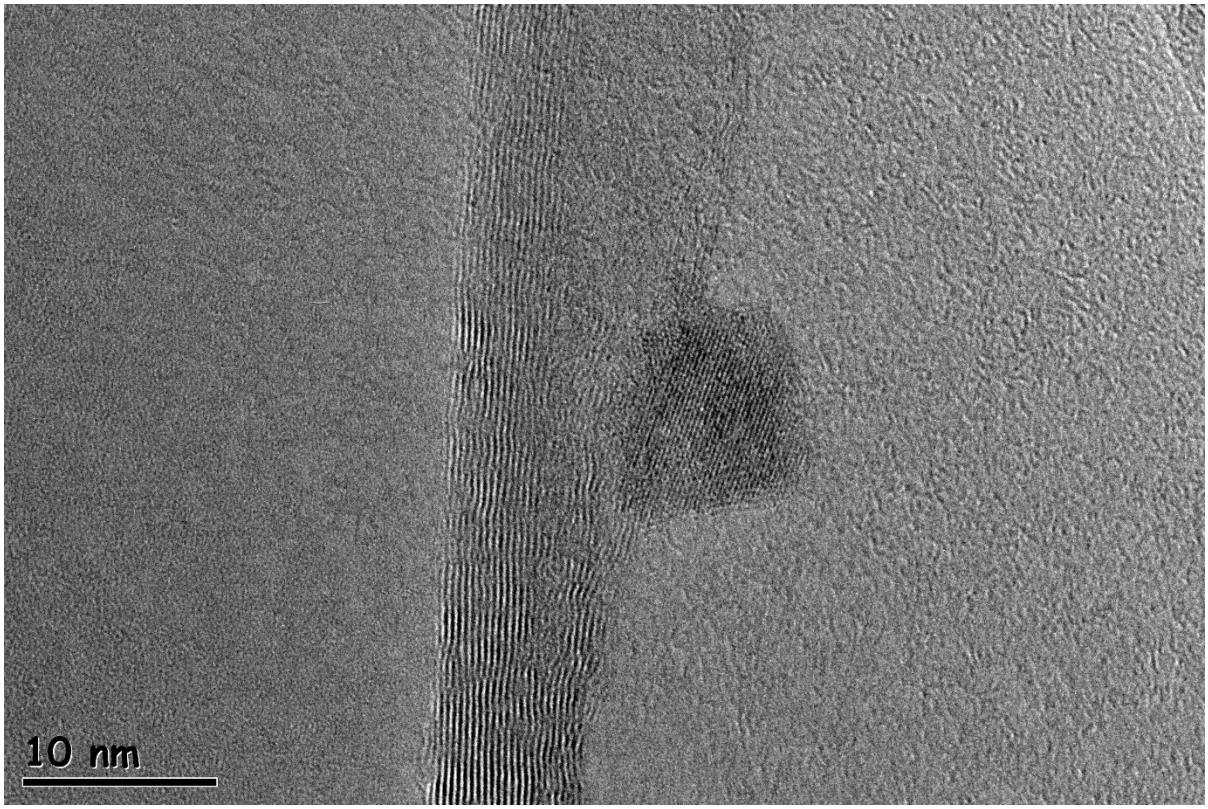

Figure 18. Fe_3O_4 nanoparticle on the MWCNT

3.1.4 Vibrating Sample Magnetometer (VSM)

Figure 17 reveals that 3 hysteresis lines pass through the origin which explains that all three substances (25% Fe_3O_4/MWCNT, 40% Fe_3O_4/MWCNT and 50% Fe_3O_4-MWCNT) are super paramagnetic. The saturation magnetization of 40.23 emu.g^{-1}, the coercivity (H_c) and the remnant magnetization (M_r) of the sample was close to zero. This suggests superparamagnetism of Fe_3O_4/CNTs nanoparticles with practical applications in external magnetic field separations. Table 5 reports the main magnetic characterization results of the investigated samples.

Table 5. The saturation magnetization, coercivity and the remnant magnetization values for synthesized adsorbents

	Hc (T)	Mr(Emu/g)	Ms(Emu/g)
25% Fe_3O_4/MWCNT	0,0063	-1,54	13,9
40% Fe_3O_4/MWCNT	0,0064	-2,52	20,10
50%Fe_3O_4-MWCNT	0,0066	-3,47	40,23

Fig. 19 shows a representative hysteresis curve of the Fe_3O_4/MWCNT systems; a typical superparamagnetic behavior marked by a slow approach to saturation is observed. However, an ideal superparamagnetic system is also characterized by the absence of coercive field. In the curve shown in Fig. 19, a faint, non-zero value of the coercivity is found. This behavior can be ascribed to the existence of magnetic interaction among the magnetic nanoparticles due to aggregation effects. Such a hypothesis is confirmed by the TEM images shown in Fig. 17, where nanoparticles aggregation is evident resulting in higher magnetic volume with respect to the single nanoparticle.

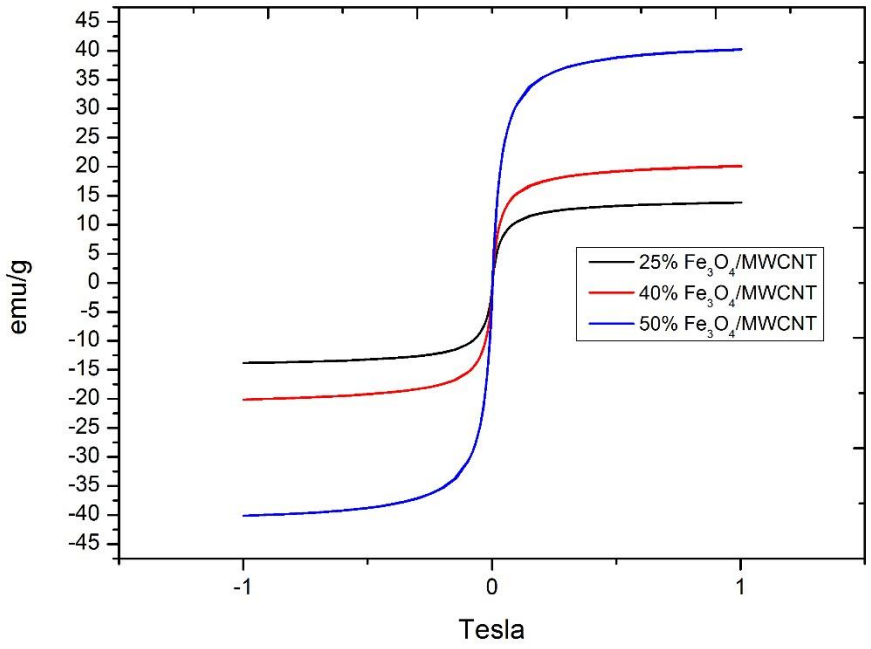

Figure 19: The magnetization hysteresis loops of Fe_3O_4/MWCNT nanoparticles

3.2 Optimization of Extraction Capacity of Nanocomposites

The surface modification of CNTs was performed to obtain better extraction of PAHs. As it was mentioned above, in this study the most abundant 6 PAHs were examined as pollutant.

The retention times of 6 PAHs to be studied were determined by applying the method described in Table 1. To determine the absolute retention time, scan mode is used primarily for GC-MS. Scan mode is used to monitor all ions using the mass detector and is used for quantitative analysis. When SIM mode is set, target ions determined in scan mode are introduced to the instrument and qualitative analysis is applied.

The spectrum obtained from analysis of standard samples by GC-MS using scan mode is shown in the figure. Identification was made by using both retention times (polarity) and target ion in mass spectrums. Library search results getting from the GC-MS instrument are attached to the Appendix.

Table 6: Retention times and target ion numbers obtained from scan mode run

Polycyclic Aromatic Hydrocarbons	***Retention Time (min)***	***Target Ion (m/z)***
Naphthalene (Nap)	11.417	128,127,129
Acenaphtene (Acy)	16.050	153, 154, 152
Acenapthylene (Ace)	16.627	152, 153, 154
Fluorene (Fle)	18.202	166,165,163
Anthracene (Ant)	21.345	178,176,179
Phenantherene (Phe)	21.495	178,176,179

The above table lists the names of the PAHs studied and associated retention times and target ions. Before the analyses of each PAH, instrument was run in scan mode to see locations of each PAH (Figure 22). Apart from these indicated peaks, other small peaks can be also seen in the spectrum. Because of the PAH solution is in the cyclohexane solvent, these small peaks belongs to the solvent, however because of these peaks cannot combine with the 6 PAHs can easily eliminate with the background subtraction. Figure 23 shows the mass spectra of 6 PAHs.

Quality control studies for analytical measurements are performed in terms of accuracy and precision. To understand how calibrated to the instrument 0.1, 0.3, 0.5, 0.8 and 1.0 ppm solutions were prepared from the standard and the calibration curve was plotted according to the response of these solutions. As it can be seen from the graphs, calibration curves are quite reasonable to continue for the analysis.

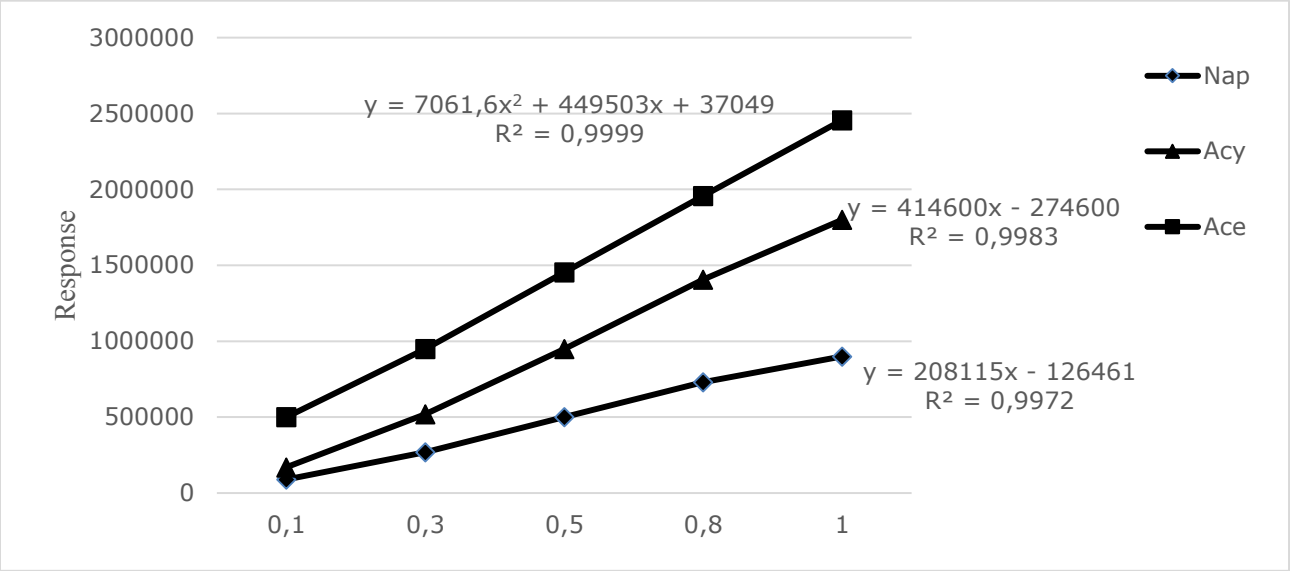

Figure 20: Calibration curves of Nap, Acy and Ace

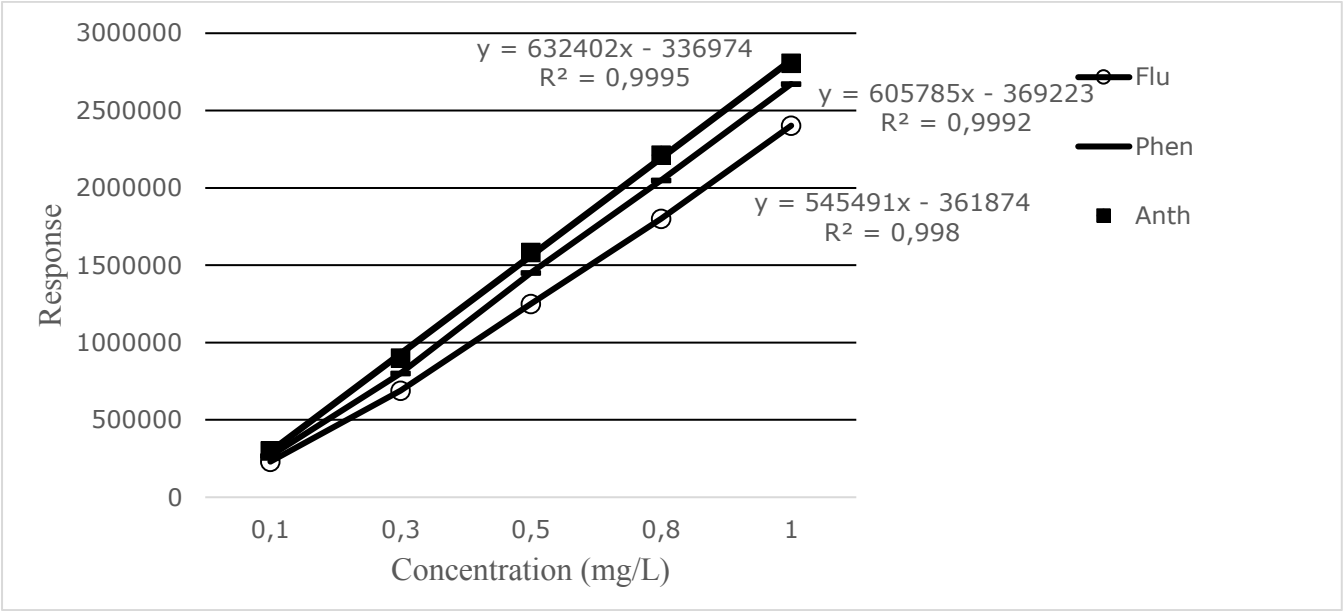

Figure 21: Calibration curves for Flu, Anth and Phe

Limit of Detection (LOD) was calculated as 3s/m formula. “s” is the standard deviation of the response using an analyte concentration close to LOQ and “m” is the slope of the calibration curve.

Table 7: LOD and LOQ values of studied PAHs

PAHs	Limit of Detection(LOD)ppb	Limit of Quantification (LOQ)ppb
Naphthalene (Nap)	0.0980	0.327
Acenaphtylene(Acy)	0.0560	0.187
Acenaphtene (Ace)	0.0250	0.0833
Fluorene (Flu)	0.0370	0.123
Phenanthrene (Phe)	0.0390	0.130
Anthracene (Ant)	0.0250	0.0833

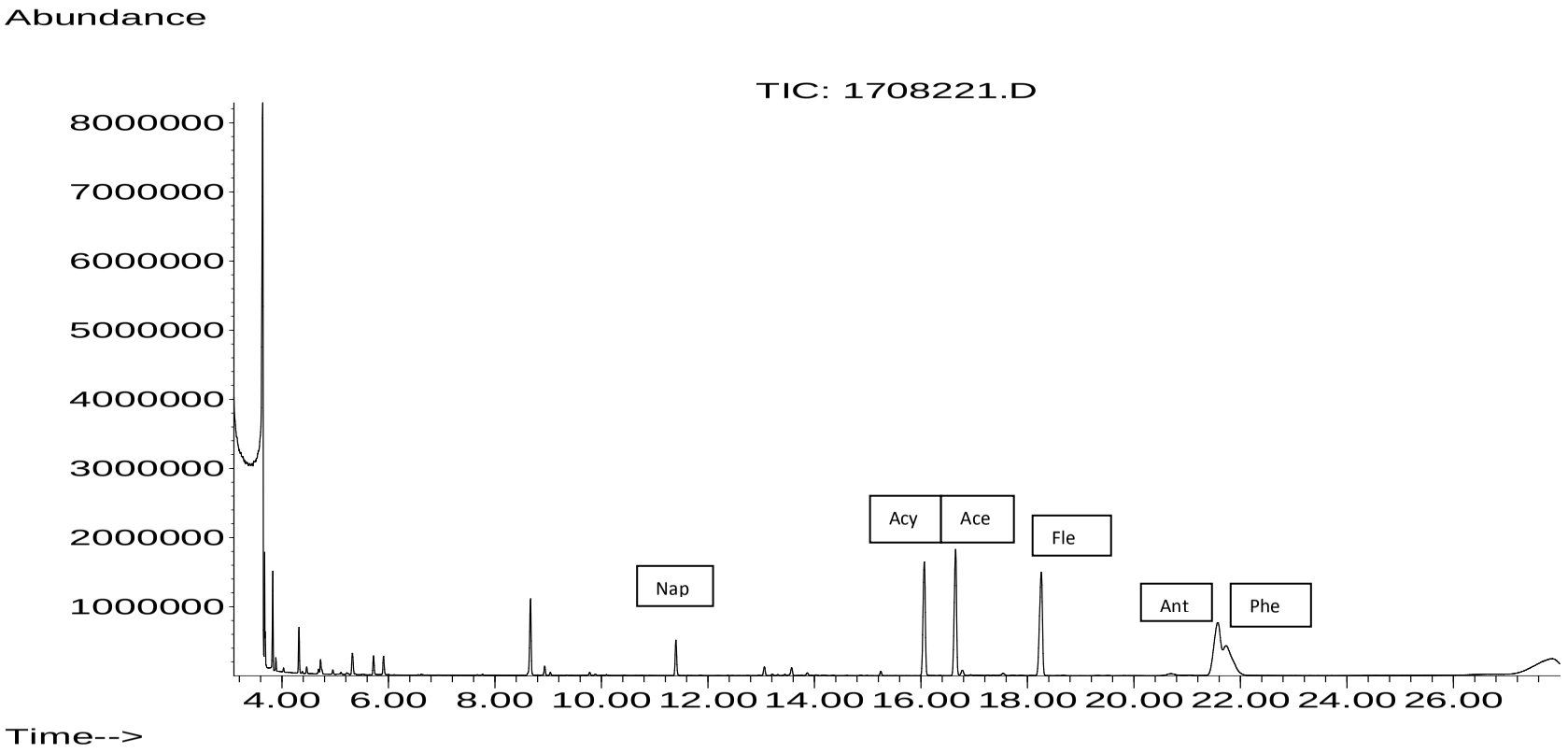

Figure 22: Scan mode spectrum of PAH standard

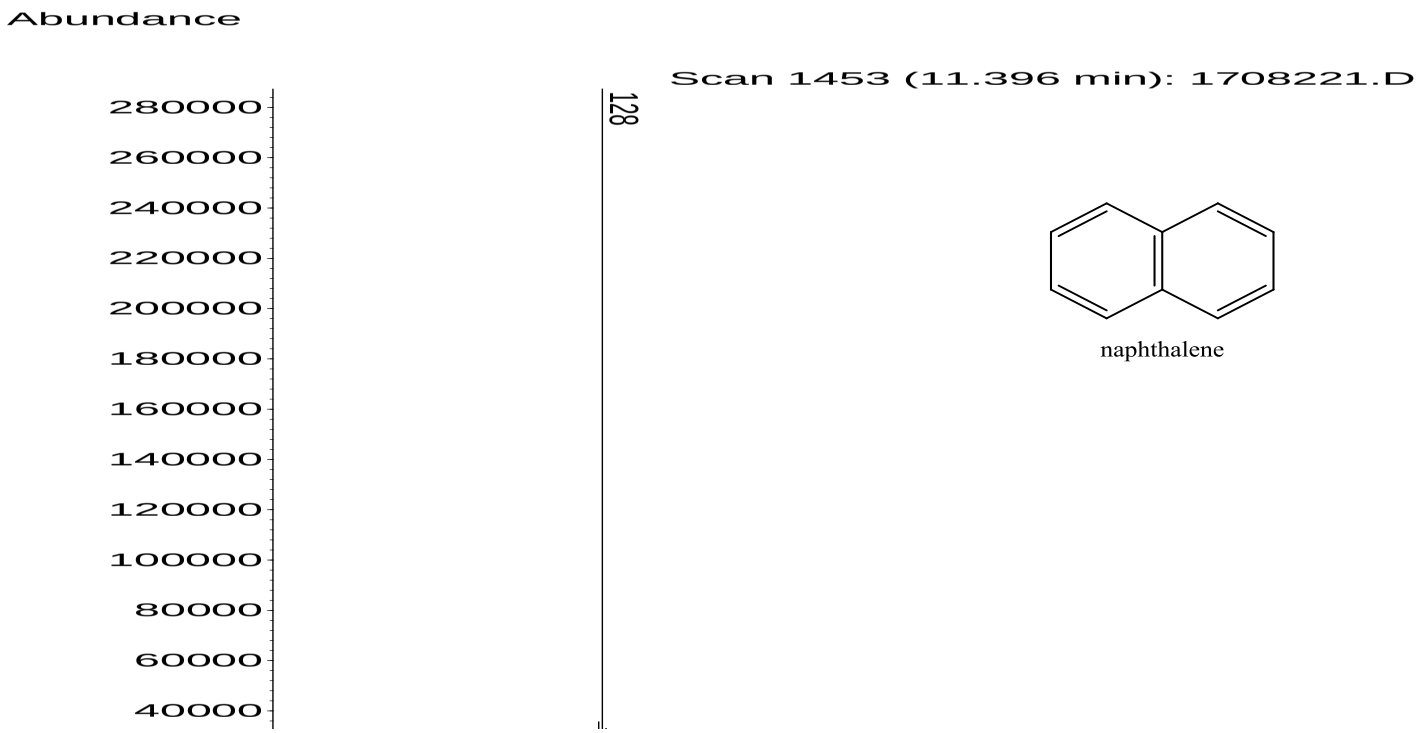

Figure 23: Mass spectrum for Naphthalene

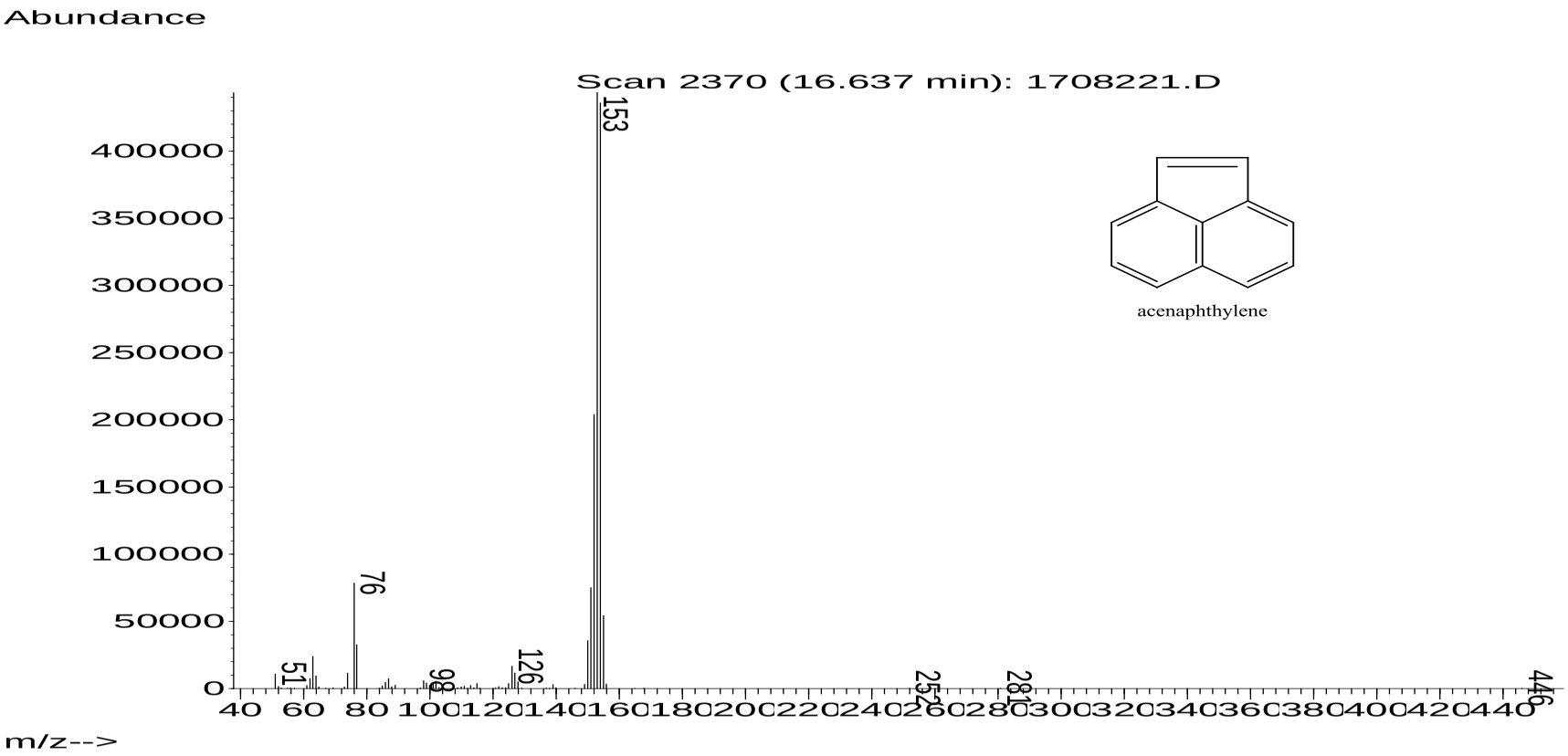

Figure 24: Mass spectrum for Acenaphtylene

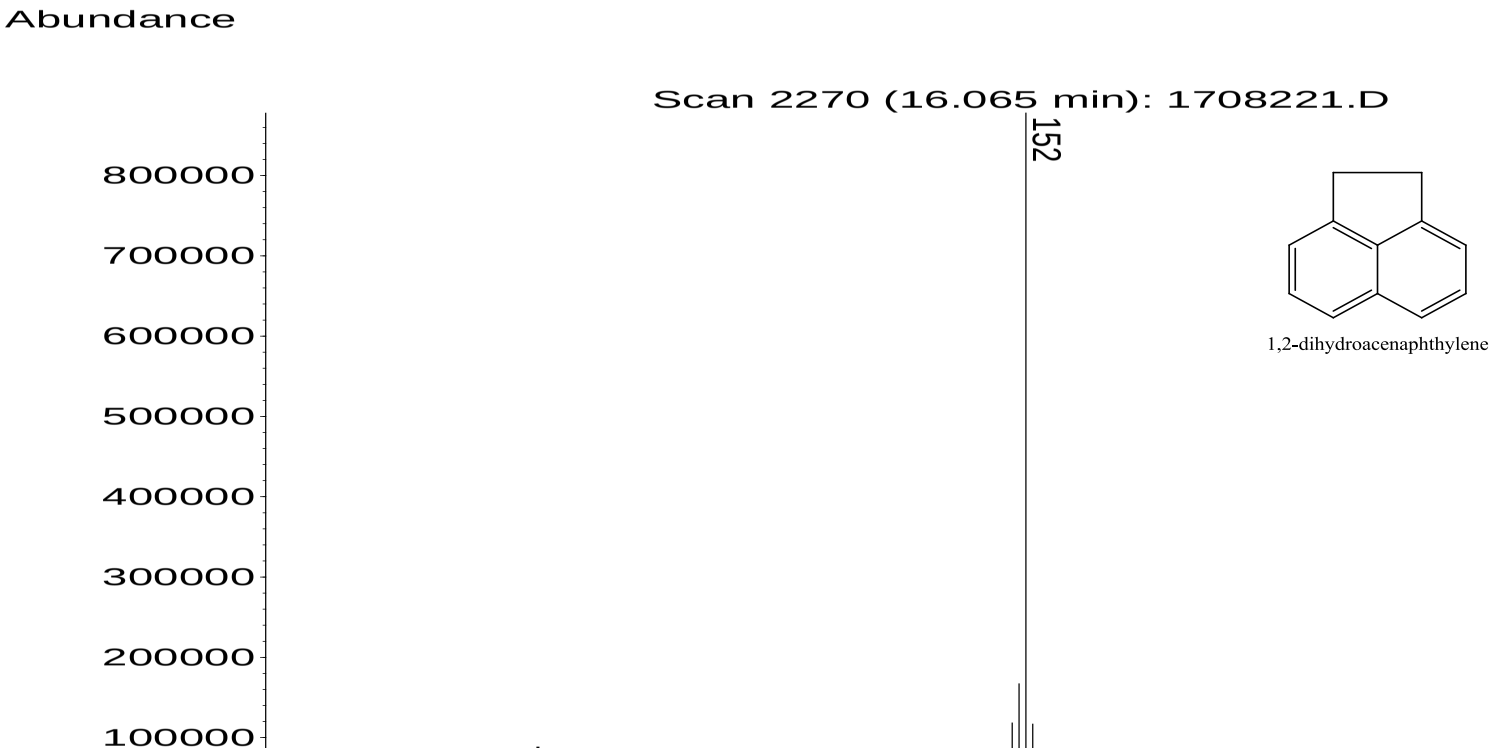

Figure 25: Mass spectrum for Acenaphthene

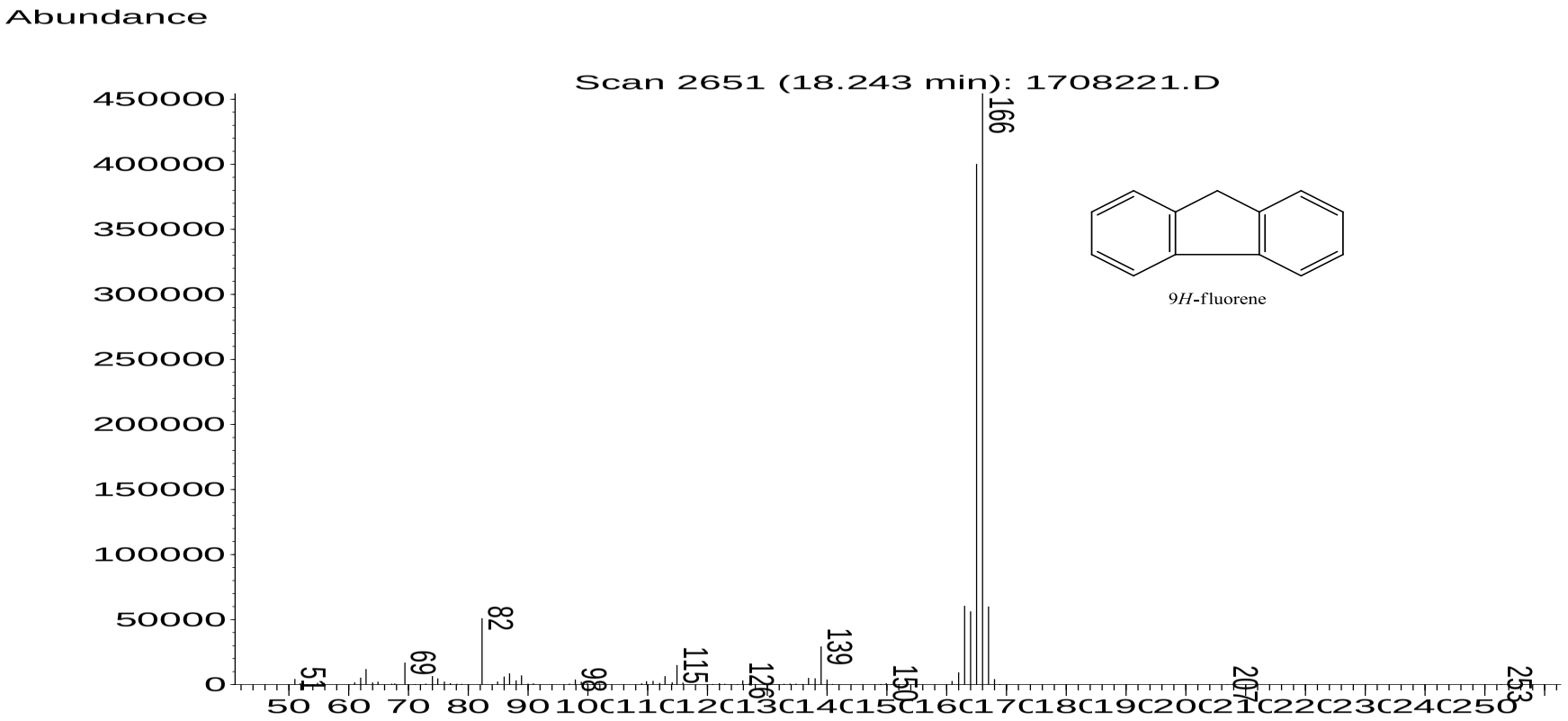

Figure 26: Mass Spectrum for Fluorene

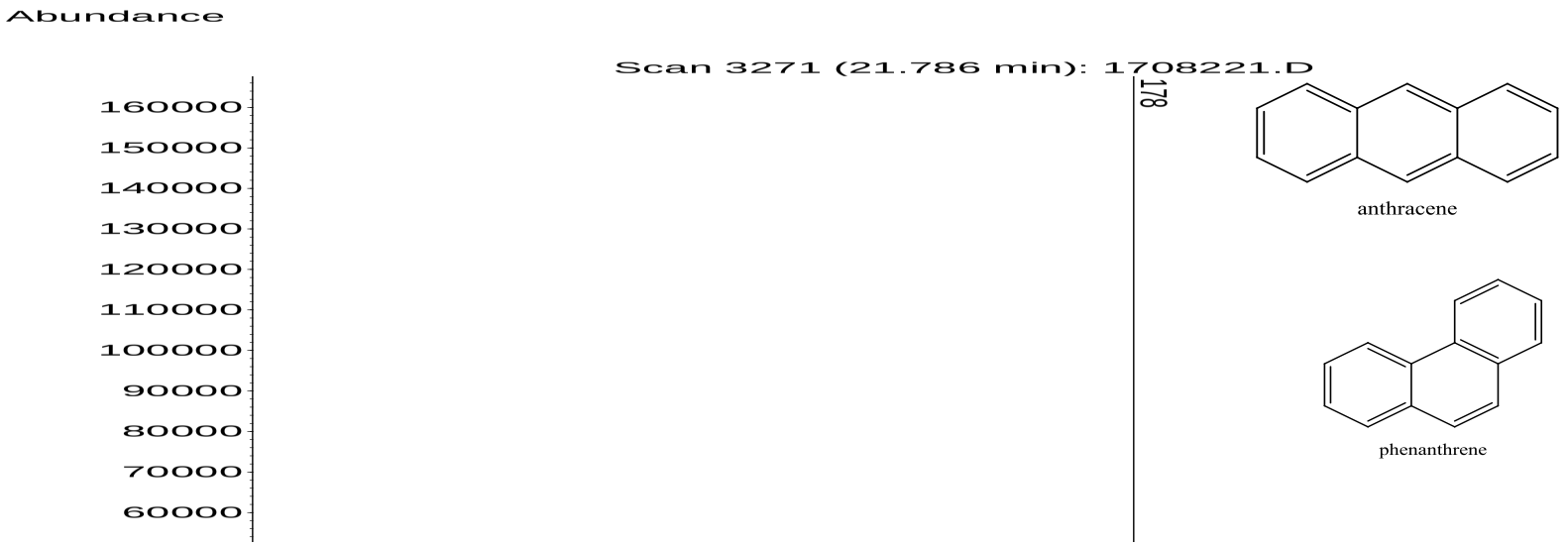

Figure 27: Mass spectrum for Anthracene and Phenanthrene

3.3 Optimization of Extraction Capacity

Optimization experiments were performed starting first with MWCNT and afterwards with each composite. Best removal was tried to achieve by optimizing amount of adsorbent and contact time.

Adsorbed amounts of the compounds were calculated from the difference between areas of the peaks obtained before and after the treatment of standards. Adsorption efficiencies were calculated with following equation:

$$\text{Adsorption efficiency (\%)} = \frac{adsorbed\ amount\ (\frac{mg}{ml})}{initial\ amount\ (\frac{mg}{ml})} \times 100$$

3.3.1 Effect of Dosage

The amount of adsorbents in the water is one of the major factors, which affects the adsorption capacity. The batch adsorption experiments were carried out using various amounts of MWCNTs from 30 to 200 mg while the pH and contact time were fixed at 7 and 60 minutes, respectively. The results displayed in Figure 23 indicate that the adsorption capacity increases with increasing MWCNT dosage up to 50 mg, then remains almost constant for the remaining dosage range, 50 mg to 200 mg. For the range below 200 mg, the increase in percentage removal with the increase in dosage rate is expected because the higher the dose of MWCNT in the solution, the greater the availability of exchangeable sites for PAHs. However, after certain dosage rate, which is 50 mg in this study, the dosage rate was found to have no effect on the percentage removal.

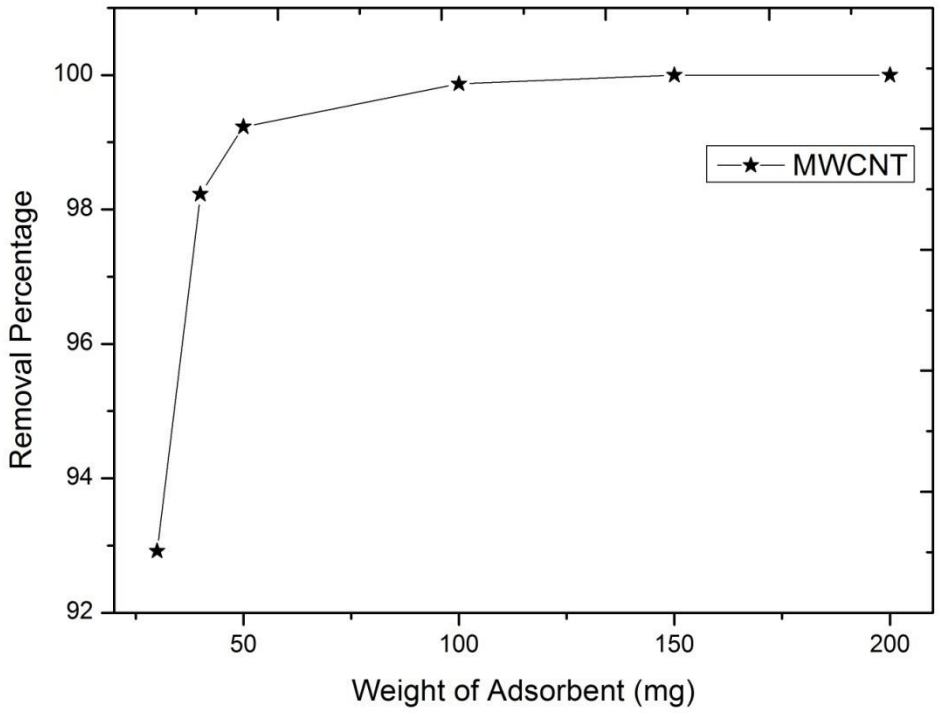

Figure 28: Effect of MWCNT dosage mass on the removal percentage

3.3.2 Effect of Contact Time

The adsorption behavior of PAHs by the MWCNT as a function of contact time was studied by varying the contact time from 1 minutes to 24 hours at a total PAH concentration of 0.5 mg/L. The results presented in Figure 24 show that, the adsorption rate reached the equilibrium for both adsorbents after two hours and the removal rates of Total PAH 98%. A slight drop in the removal percentage was obtained beyond two hours contact time because the bonds formed during the interaction break after a while.

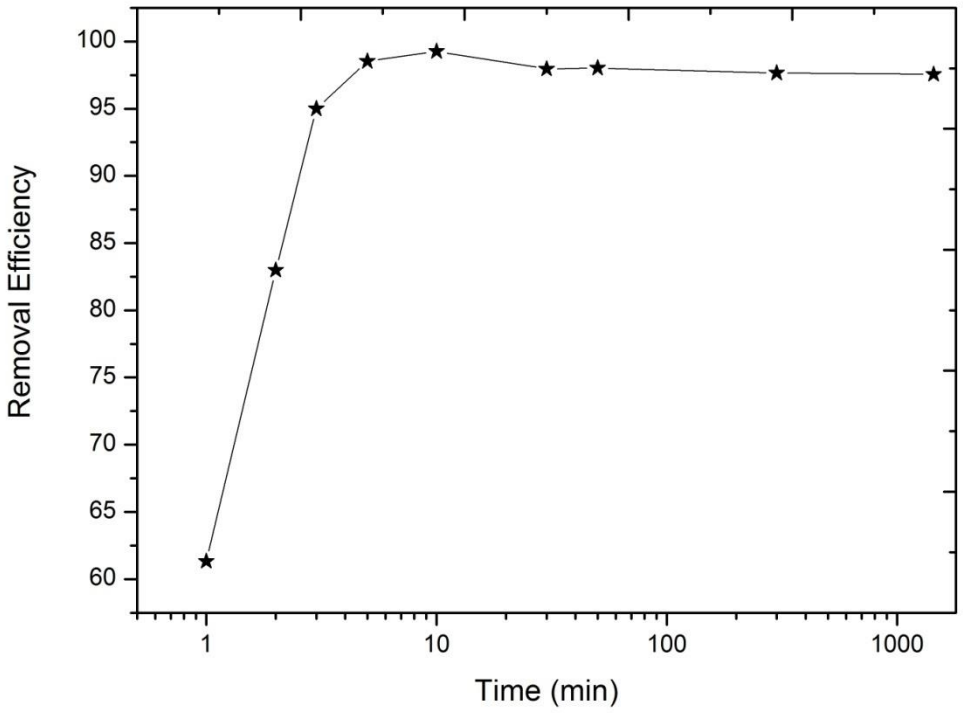

Figure 29: Effect of contact time on the removal efficiency

3.4 Adsorption of PAHs by Different Nanocomposites

The amount of PAHs adsorbed on the MWCNT, f-MWCNT and MWCNT with varying Fe_3O_4content at 10 min time interval is depicted in Figure 30.

The MWCNT interacts perfectly with PAH. When the removal efficiencies of different materials were examined, MWCNT adsorbed PAHs very quickly and efficiently because of π - π interaction between them.

It can be clearly seen that first 5 minute is very important for the adsorption process. Figure 25 shows the ∑6 PAHs' removal efficiencies on different adsorbents during 24 hours. The slowest adsorption occurs on the 50% Fe_3O_4/MWCNT because of the steric effect prevent to be formed π– π interaction between PAHs and MWCNT. 40% Fe_3O_4/MWCNT is the other slowest adsorbent due to the same reason.

While it was anticipated that the fastest adsorption process would occur on MWCNT, 25% Fe_3O_4/MWCNT gives best removal efficiency in the shortest time. For this reason, 25% Fe_3O_4/MWCNT forestalled MWCNT not only

because of its excellent adsorption property but also because of its magnetic property.

At the 300th minute, all PAH molecules are liberated from steric hindrence and show the same removal efficiencies on all adsorbents, because all nanocomposites contain the same amount of MWCNT. This study shows that no matter how much Fe_3O_4 is deposited on the MWCNT, new composite do not show worse adsorption in the long term, on the contrary, this process adds a strong magnetic property to MWCNT, which is a very important feature of environmental remediation molecules.

Being an adsorbent with magnetic properties makes Fe3O4-MWCNT a superior material because one of the recently discussed and worried topics is the release of too much carbon nanotubes into the environment. Unfortunately, MWCNT alone cannot be recycled when used in adsorption, but after Fe3O4-MWCNT adsorb the PAHs, it can be easily cleaned from the environment with a simple magnet.

Figure 31, 32, 33 and 34 shows the individual PAHs' trends for removal efficiency.

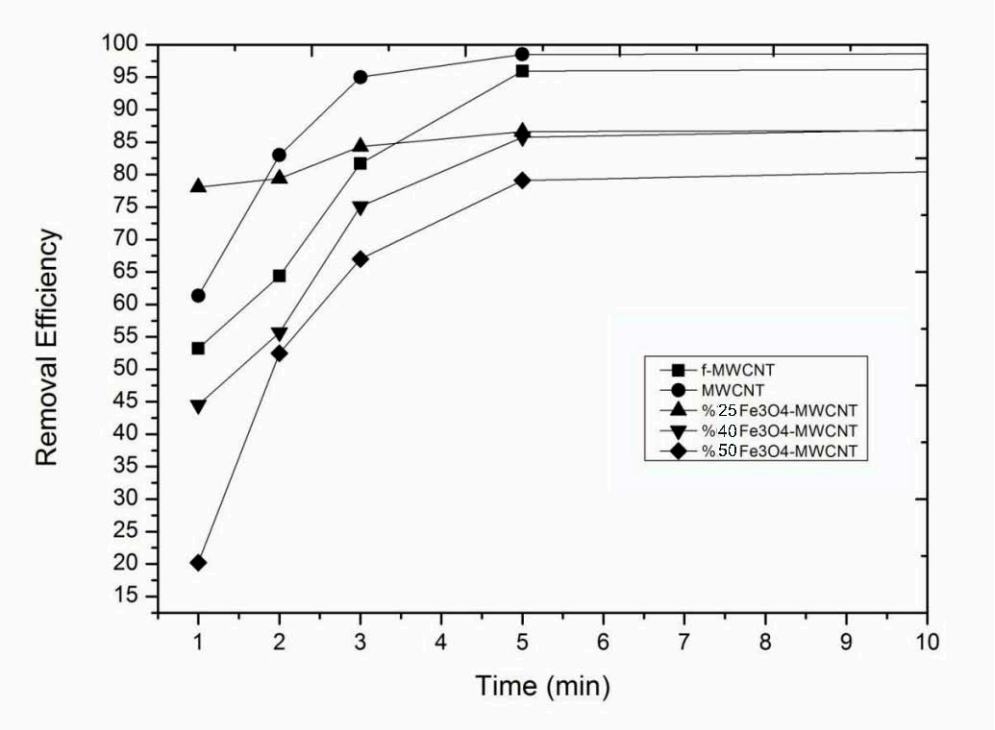

Figure 30: First 10 minutes into the adsorption process

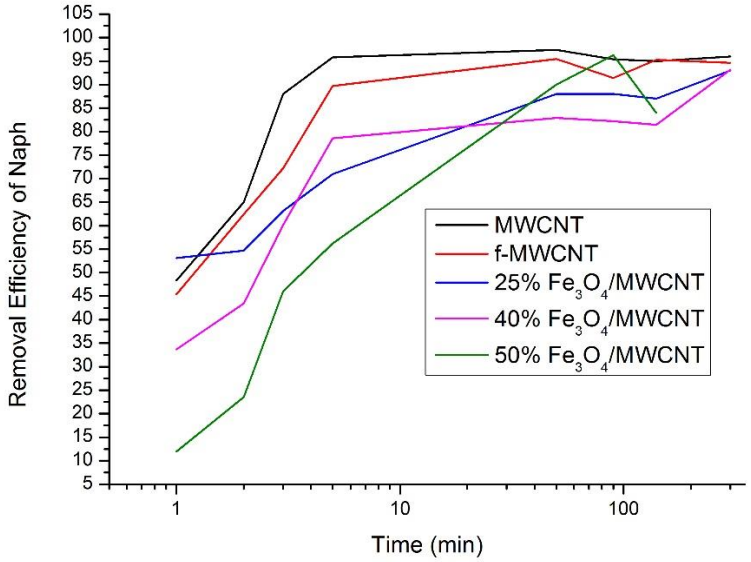

Figure 31. Removal Efficiencies of naphthalene on different adsorbents

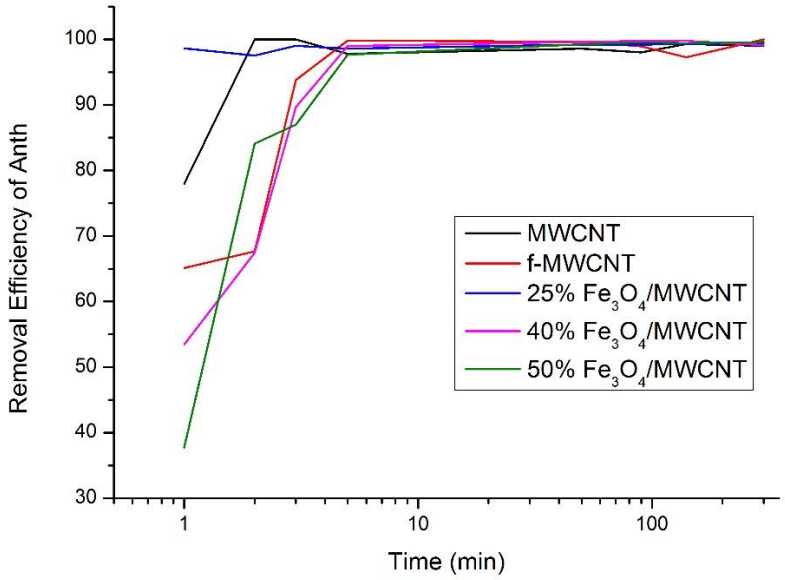

Figure 32. Removal Efficiencies of anthracene on different adsorbents

Figure 30: First 10 minutes into the adsorption process

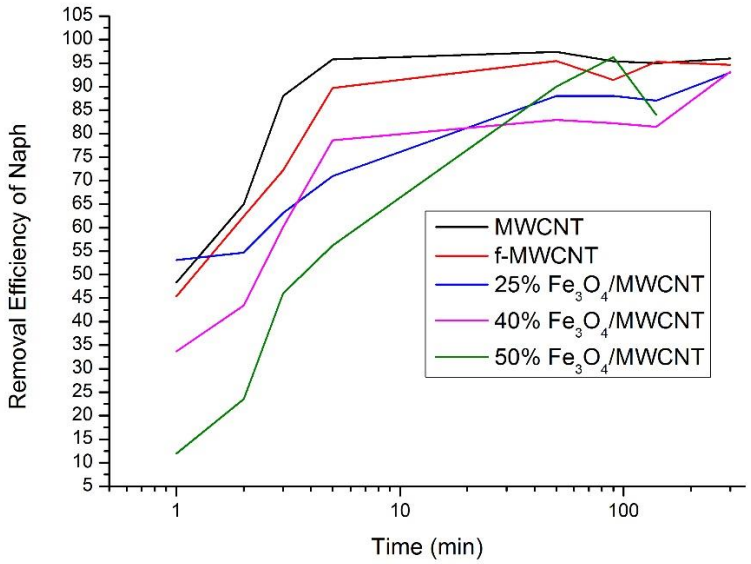

Figure 31. Removal Efficiencies of naphthalene on different adsorbents

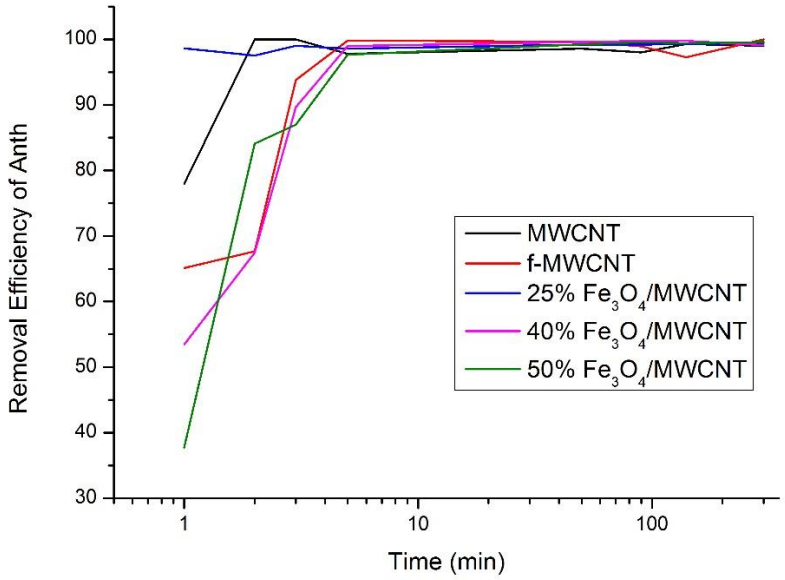

Figure 32. Removal Efficiencies of anthracene on different adsorbents

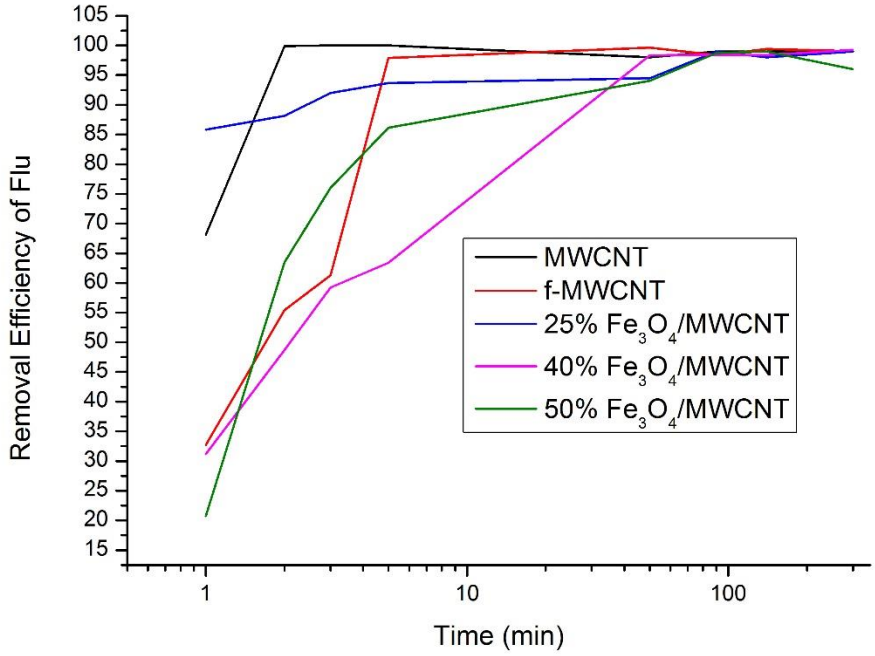

Figure 33. Removal Efficiencies of fluorene on different adsorbents

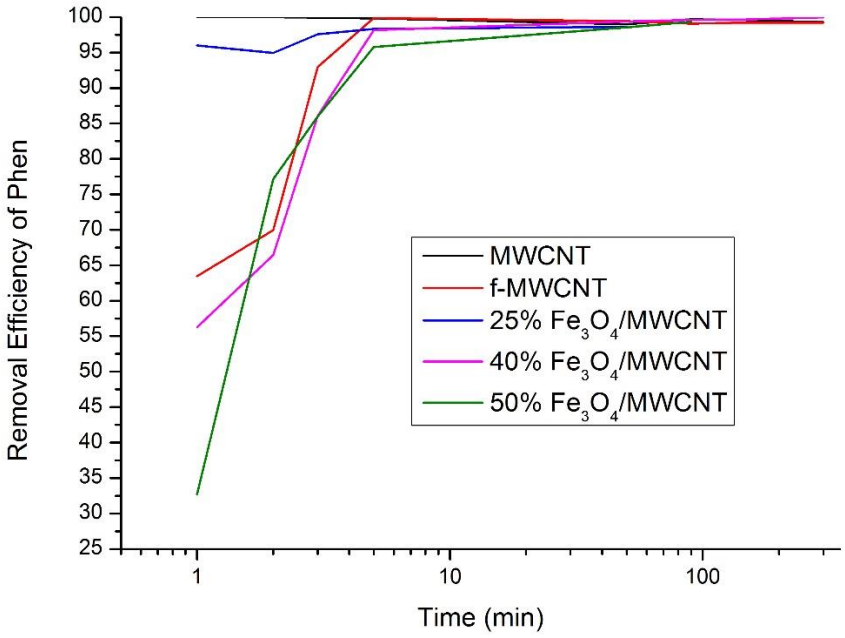

Figure 34. Removal Efficiencies of phenanthrene on different adsorbents

3.5 Adsorption Isotherms

For the Freundlich gave an empirical expression representing the isothermal variation of adsorption of a quantity of PAH adsorbed by unit mass. Freundlich Adsorption Isotherms were applied for 6 PAHs and Freundlich equations were constituted.

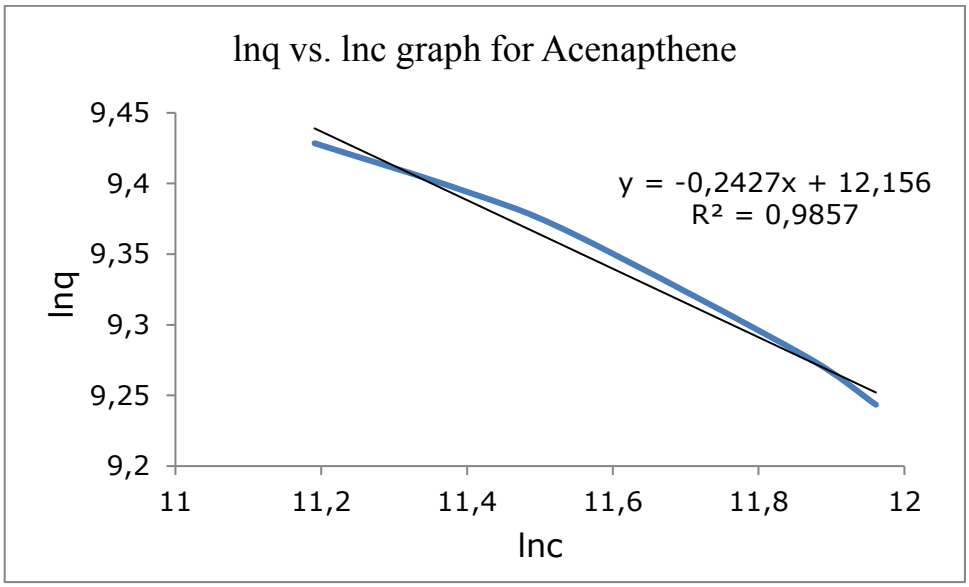

a

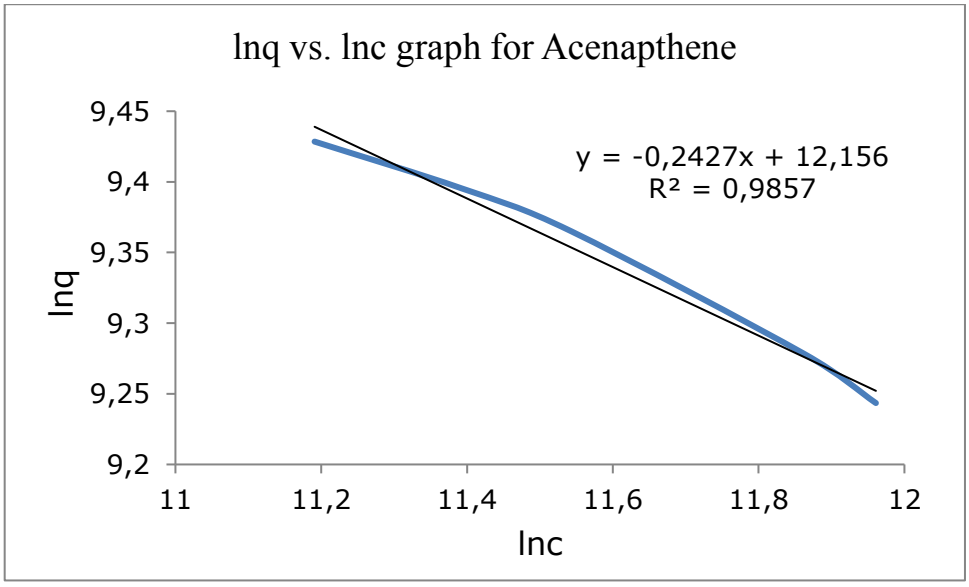

b

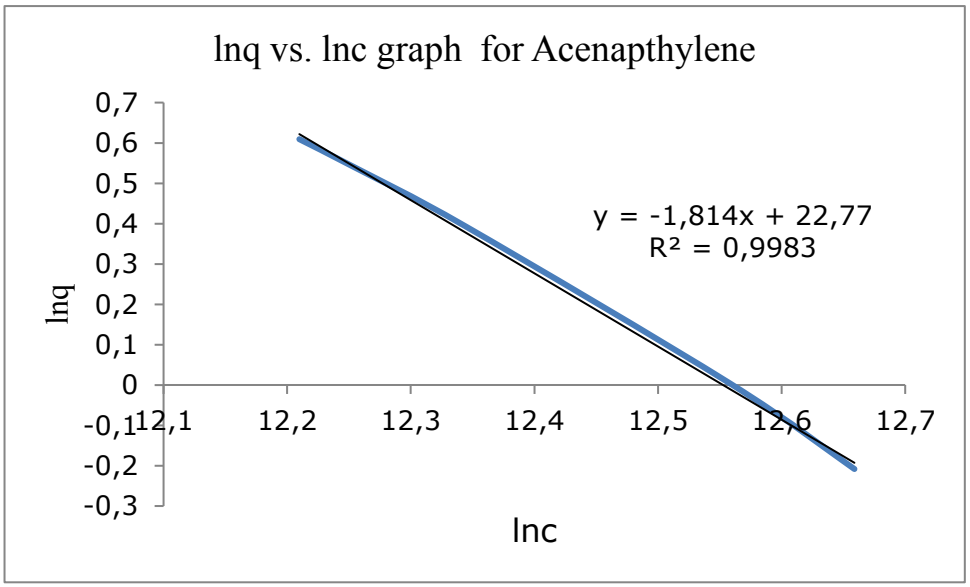
lnq vs. lnc graph for Acenapthylene
y = -1,814x + 22,77
R² = 0,9983
lnq
lnc
0,7
0,6
0,5
0,4
0,3
0,2
0,1
0
-0,1
-0,2
-0,3
12,1
12,2
12,3
12,4
12,5
12,6
12,7

c

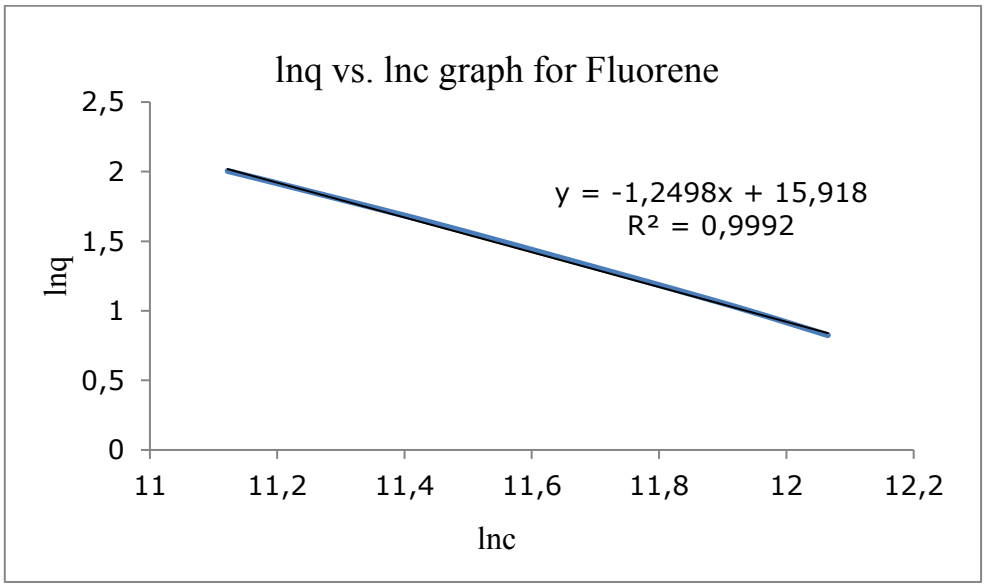
lnq vs. lnc graph for Fluorene
y = -1,2498x + 15,918
R² = 0,9992
lnq
lnc
2,5
2
1,5
1
0,5
0
11
11,2
11,4
11,6
11,8
12
12,2

d

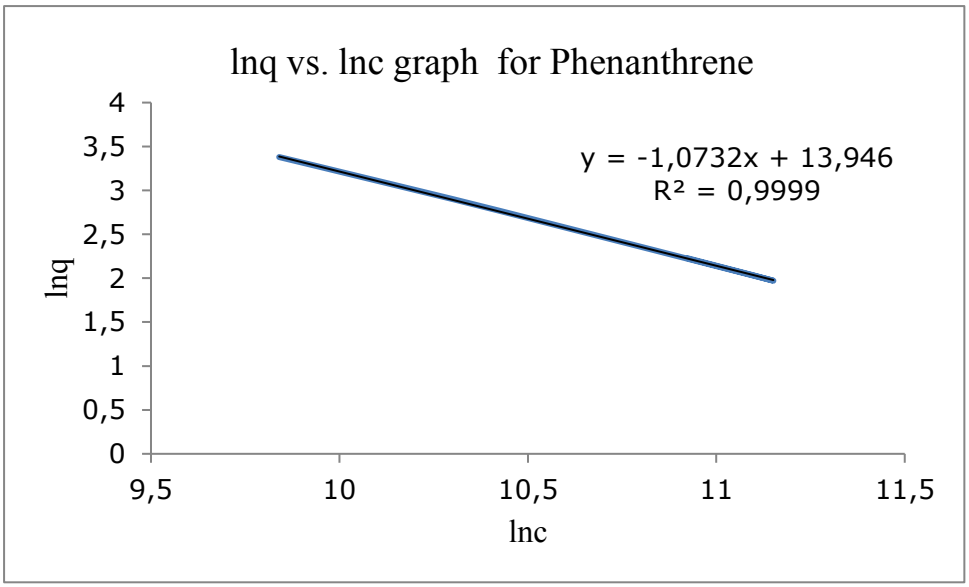

e

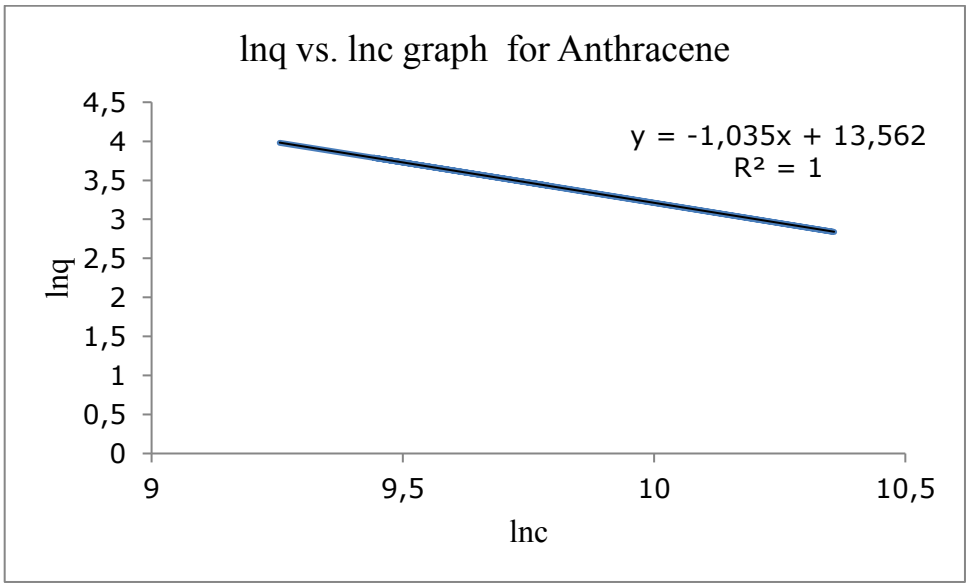

f

Figure 35. lnq vs. lnc graph for the (a) Naphthalene, (b) Acenapthene, (c) Acenapthylene, (d) Fluorene, (e) Phenanthenere and (f) Anhtracene.

According to the lnq vs. lnc graphs table 8 were set. Kf is the Freundlich constant, 1/n is the exponent of non-linearity and c represents the concentration.

Table 8. Freundlich Constants for 6 PAHs

	r^2	n	kf	Freundlich Equation
Naph	0,992	-1,7	1,27E+07	Q_e= 1,27E+07. $c^{-1/1,7}$
Ace	0,985	-4,1	1,89E+05	Q_e= 1,89E+05. $c^{-1/4,1}$
Acy	0,998	-0,6	7,74E+09	Q_e= 7,74E+09. $c^{-1/0,6}$
Flu	0,999	-0,8	8,12E+06	Q_e= 8,12E+06. $c^{-1/0,8}$
Phen	0,999	-0,9	1,13E+06	Q_e= 1,13E+06. $c^{-1/0,9}$
Anth	1,000	-1,0	7,75E+05	Q_e= 7,75E+05. $c^{-1/1,0}$

3.6 Magnetic Property of Fe3O4/MWCNT Nanoparticles

The magnetic properties of Fe3O4 particles, which have been proven for their excellent adsorption ability, have also been investigated, which is another advantage of using these particles in wastewater. Magnetic separation is very important for these nanoparticles to recover after cleaning up the contaminated water. The Fe_3O_4/MWCNT nanoparticles adsorb both the toxic PAHs to almost MWCNT and allow them to easily separate from the water after adsorption. Figure 30 show how the Fe_3O_4 nanoparticles are recovered after the adsorption process. When the percentages of the Fe increases, recovery velocity also increases. When pH 7, although 25% Fe_3O_4/MWCNT can be collect with a magnet in 17 minutes, 50% Fe_3O_4/MWCNT can be collect completely in 6 minutes.


400
APPROX
400 ml
Boro 3.3
240
160
80


160
80


160
80

Figure 36: Recovering of Fe_3O_4/MWCNTs from the solution

CHAPTER 4

CONCLUSION

This work introduces magnetic Fe_3O_4-MWCNT nanoparticles that can be used for the environmental remediation of toxic PAHs. Within the scope of the study, three materials were synthesized at different percentages: 25% Fe_3O_4/MWCNT, 40% Fe_3O_4/MWCNT and 50% Fe_3O_4/MWCNT. The synthesized nanoparticles were characterized with FT-IR, XRD, VSM and TEM instruments and results showed that nanomaterials has been synthesized successfully and they exhibit superparamagnetic properties with a saturation magnetization of 40.23emu.g^{-1}. XRD results exhibit that Fe_3O_4-MWCNT nanoparticle has the spinal phase structure and FT-IR spectra reveal that Fe-O-Fe stretching can be observed in the molecule. According to the TEM analysis, average Fe_3O_4 particle has 9 nm size. For the GC-MS calibration, naphthalene, acenapthalene, acenapthyne, fluorene, phenantherene and anthracene r^2 values are 0,999, 0,998, 0,997, 0,999, 0,999 and 0,998, respectively.

Fe_3O_4-MWCNT nanoparticles not only give excellent removal efficiencies but also move one step further than other adsorbents due to their magnetic properties. It is easy to remove the adsorbent from the solution. To observe the change in adsorption percentages over time 6 PAHs were selected. Decrease in the Fe_3O_4 content causes the increase in the adsorption efficiency because Fe_3O_4 causes steric hindrance around the MWCNT and prevents the bond formation between MWCNT and PAHs.

Increase in the Fe_3O_4 content causes the stronger magnetic property, which may be desired in the fast water remediation situations.

As a future work, the synthesis method can be extended for depositing other organic and inorganic pollutants onto Fe_3O_4-MWCNT using appropriate precursors and solvents. Moreover, because of the magnetic nanoparticles are reusable, desorption studies will be done in the near future. Considering the recent studies on the using Fe_3O_4-MWCNT for various applications like biomedical applications, targeted drug delivery, and environmental remediation, it can be hoped that, in the nearest future, magnetic nanocomposites pose great developments in many fields.

REFERENCES

[1] H. Hung *et al.*, "Temporal trends of Persistent Organic Pollutants (POPs) in arctic air: 20 years of monitoring under the Arctic Monitoring and Assessment Programme (AMAP)," *Environ. Pollut.*, vol. 217, pp. 52–61, 2016.

[2] M. Ligaray, S. S. Baek, H.-O. Kwon, S.-D. Choi, and K. H. Cho, "Watershed-scale modeling on the fate and transport of polycyclic aromatic hydrocarbons (PAHs)," *J. Hazard. Mater.*, vol. 320, pp. 442–457, Dec. 2016.

[3] L. Xu, J. Li, and M. Zhang, "Adsorption characteristics of a novel carbon-nanotube-based composite adsorbent toward organic pollutants," *Ind. Eng. Chem. Res.*, vol. 54, no. 8, pp. 2379–2384, 2015.

[4] H. Wu *et al.*, "Persistent organic pollutants and type 2 diabetes: A prospective analysis in the nurses' health study and meta-analysis," *Environ. Health Perspect.*, vol. 121, no. 2, pp. 153–161, 2013.

[5] E. Emeville, A. Giusti, X. Coumoul, J.-P. Thomé, P. Blanchet, and L. Multigner, "Associations of Plasma Concentrations of Dichlorodiphenyldichloroethylene and Polychlorinated Biphenyls with Prostate Cancer: A Case–Control Study in Guadeloupe (French West Indies)," *Environ. Health Perspect.*, no. January, Nov. 2014.

[6] L. J.-E. and J. S.H., "Association between serum levels of adiponectin and polychlorinated biphenyls in Korean men and women," *Endocrine*, pp. 211–217, 2014.

[7] R. Liu, D. O. Nelson, S. Hurley, A. Hertz, and P. Reynolds, "Residential Exposure to Estrogen Disrupting Hazardous Air Pollutants and Breast Cancer Risk," *Epidemiology*, vol. 26, no. 3, pp. 365–373, May 2015.

[8] "Modification , Development and Application of Extraction Methods For PAHs in Sediments and Water by Precious Nokwethemba Sibiya A thesis submitted to the Faculty of Science , University of the Witwatersrand , Johannesburg , in fulfillment of the requirem," 2012.

[9] G. Karaca, "Spatial Distribution of Polycyclic Aromatic Hydrocarbon (PAH) Concentrations in Soils from Bursa, Turkey," *Arch. Environ. Contam. Toxicol.*, vol. 70, no. 2, pp. 406–417, 2016.

[10] B. Pan and B. Xing, "Adsorption mechanisms of organic chemicals on carbon nanotubes," *Environ. Sci. Technol.*, vol. 42, no. 24, pp. 9005–9013, 2008.

[11] B. Glomstad *et al.*, "Evaluation of methods to determine adsorption of polycyclic aromatic hydrocarbons to dispersed carbon nanotubes," *Environ. Sci. Pollut. Res.*, 2017.

[12] E. O. Gaga, G. Tuncel, and S. G. Tuncel, "Sources and Wet Deposition Fluxes of Polycyclic Aromatic Hydrocarbons (PAHs) in an Urban Site 1000 Meters High in Central Anatolia (Turkey)," *Environ. Forensics*, vol. 10, no. 4, pp. 286–298, 2009.

[13] S. G. Tuncel and T. Topal, "Multifactorial Optimization Approach for Determination of Polycyclic Aromatic Hydrocarbons in Sea Sediments of Turkish Mediterranean Coast," *Am. J. Anal. Chem.*, vol. 2, no. 7, pp. 783–794, 2011.

[14] B. Cetin, S. Yurdakul, M. Keles, I. Celik, F. Ozturk, and C. Dogan, "Atmospheric concentrations, distributions and air-soil exchange tendencies of PAHs and PCBs in a heavily industrialized area in Kocaeli, Turkey," *Chemosphere*, vol. 183, no. x, pp. 69–79, 2017.

[15] Y. Dumanoglu, E. O. Gaga, E. Gungormus, S. C. Sofuoglu, and M. Odabasi, "Spatial and seasonal variations, sources, air-soil exchange, and carcinogenic risk assessment for PAHs and PCBs in air and soil of Kutahya, Turkey, the

province of thermal power plants," *Sci. Total Environ.*, vol. 580, pp. 920–935, Feb. 2017.

[16] E. O. Gaga, A. Ari, T. Döğeroğlu, E. E. Çakırca, and N. E. Machin, "Atmospheric polycyclic aromatic hydrocarbons in an industrialized city, Kocaeli, Turkey: study of seasonal variations, influence of meteorological parameters and health risk estimation.," *J. Environ. Monit.*, vol. 14, no. 8, pp. 2219–29, 2012.

[17] F. Telli-Karakoç, L. Tolun, B. Henkelmann, C. Klinn, O. Okay, and K.-W. Schramm, "Polycyclic aromatic hydrocarbons (PAHs) and polychlorinated biphenyls (PCBs) distributions in the Bay of Marmara sea: Izmit Bay.," *Environ. Pollut.*, vol. 119, pp. 383–397, 2002.

[18] S. S. Cindoruk, A. Birgül, F. Esen, Y. Tasdemir, "Bursa'da Yarıkırsal Bir Bölge'de Poliklorlu Bifeniller, Organoklorlu Pestisitler ve Polisiklik Aromatik Hidrokarbonların Toplam Çökelme Akılarının Belirlenmesi", *Hava Kirliliği Araştırmaları Dergisi*, vol. 1, pp. 10–18, 2012.

[19] C. Parinos and A. Gogou, "Suspended particle-associated PAHs in the open eastern Mediterranean Sea: Occurrence, sources and processes affecting their distribution patterns," *Mar. Chem.*, vol. 180, pp. 42–50, 2016.

[20] R. K. Rajpara, D. R. Dudhagara, J. K. Bhatt, H. B. Gosai, and B. P. Dave, "Polycyclic aromatic hydrocarbons (PAHs) at the Gulf of Kutch, Gujarat, India: Occurrence, source apportionment, and toxicity of PAHs as an emerging issue," *Mar. Pollut. Bull.*, vol. 119, no. 2, pp. 231–238, Jun. 2017.

[21] B. Liu, Z. Xue, X. Zhu, and C. Jia, "Long-term trends (1990–2014), health risks, and sources of atmospheric polycyclic aromatic hydrocarbons (PAHs) in the U.S.," *Environ. Pollut.*, vol. 220, pp. 1171–1179, Jan. 2017.

[22] R. Das, S. B. Abd Hamid, M. E. Ali, A. F. Ismail, M. S. M. Annuar, and S.

Ramakrishna, “Multifunctional carbon nanotubes in water treatment: The present, past and future,” *Desalination*, vol. 354, no. December, pp. 160–179, 2014.

[23] N. Rastkari and R. Ahmadkhaniha, “Magnetic solid-phase extraction based on magnetic multi-walled carbon nanotubes for the determination of phthalate monoesters in urine samples,” *J. Chromatogr. A*, vol. 1286, pp. 22–28, 2013.

[24] S. Zeng, Y. Cao, W. Sang, T. Li, N. Gan, and L. Zheng, “Enrichment of polychlorinated biphenyls from aqueous solutions using Fe3O4 grafted multiwalled carbon nanotubes with poly dimethyl diallyl ammonium chloride,” *Int. J. Mol. Sci.*, vol. 13, no. 5, pp. 6382–6398, 2012.

[25] T. Tunçal and O. Uslu, “Industrial sludge remediation with photonic treatment using Ti-Ag nano-composite thin films: Persistent organic pollutant removal from sludge matrix,” *J. Environ. Manage.*, vol. 149, pp. 37–45, 2015.

[26] N. Chauhan and C. S. Pundir, “An amperometric biosensor based on acetylcholinesterase immobilized onto iron oxide nanoparticles/multi-walled carbon nanotubes modified gold electrode for measurement of organophosphorus insecticides,” *Anal. Chim. Acta*, vol. 701, no. 1, pp. 66–74, 2011.

[27] S. Kumar, S. Chaudhary, and J. Deep Chand, “Vibrational Studies Of Different Human Body Disorders Using FTIR Spectroscopy,” *Open J. Appl. Sci.*, vol. 4, no. 3, pp. 103–129, 2014.

[28] “Süperparamanyetik NanoManyetit.çeren LateksEldesi VeKarakterizasyonu,” Doctoral Dissertation, Balıkesir University, 2009

[29] C. T. K. H. Stadtlander, “Scanning Electron Microscopy and Transmission Electron Microscopy of Mollicutes : Challenges and Opportunities,” *Mod. Res. Educ. Top. Microsc.*, pp. 122–131, 2007.

[30] S. A. Aseyev, P. M. Weber, and A. A. Ischenko, “Ultrafast Electron Microscopy for Chemistry, Biology and Material Science,” *J. Anal. Sci. Methods Instrum.*, vol. 3, no. 1, pp. 30–53, 2013.

APPENDICES

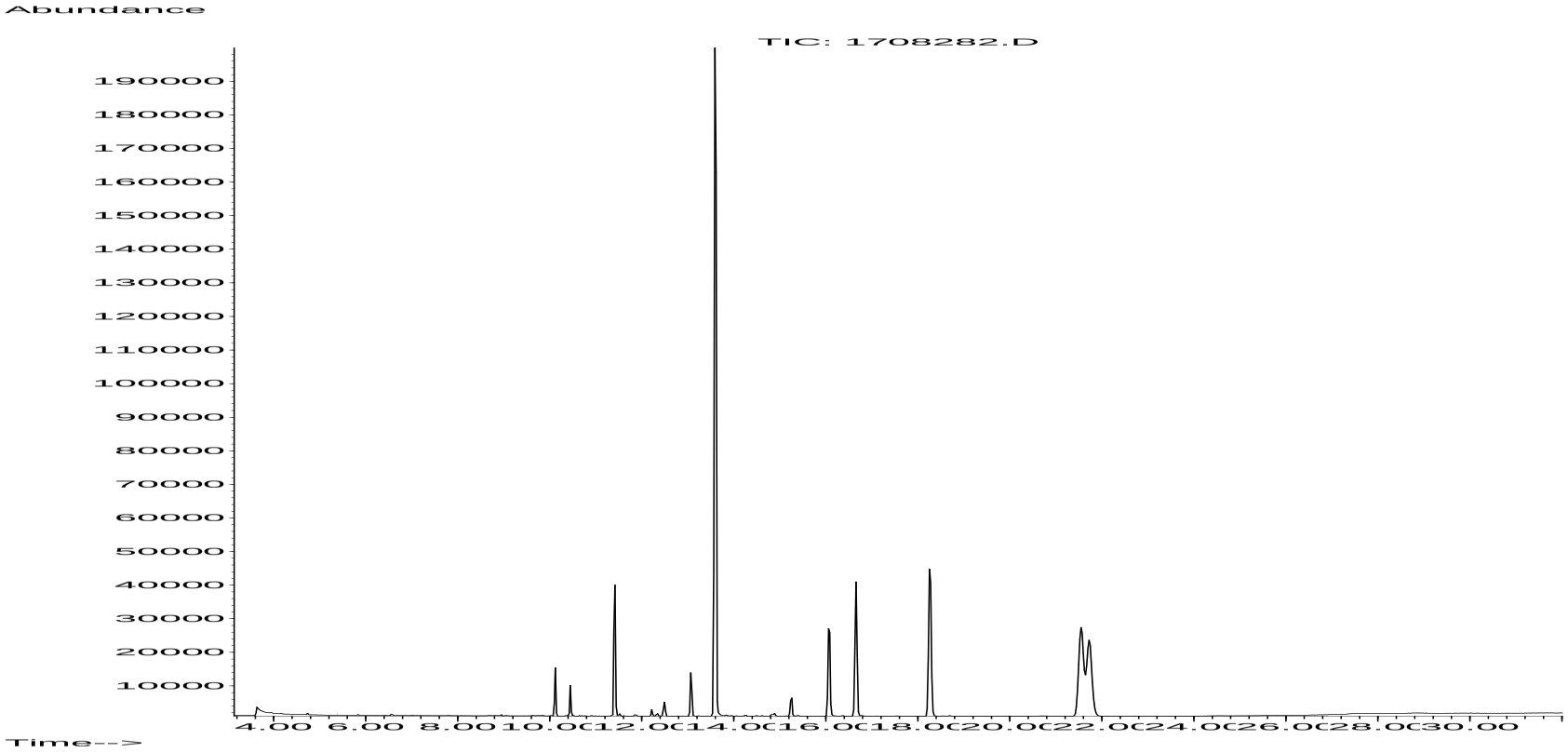

Figure 37: SIM MODE analysis of 0.5 ppm PAH

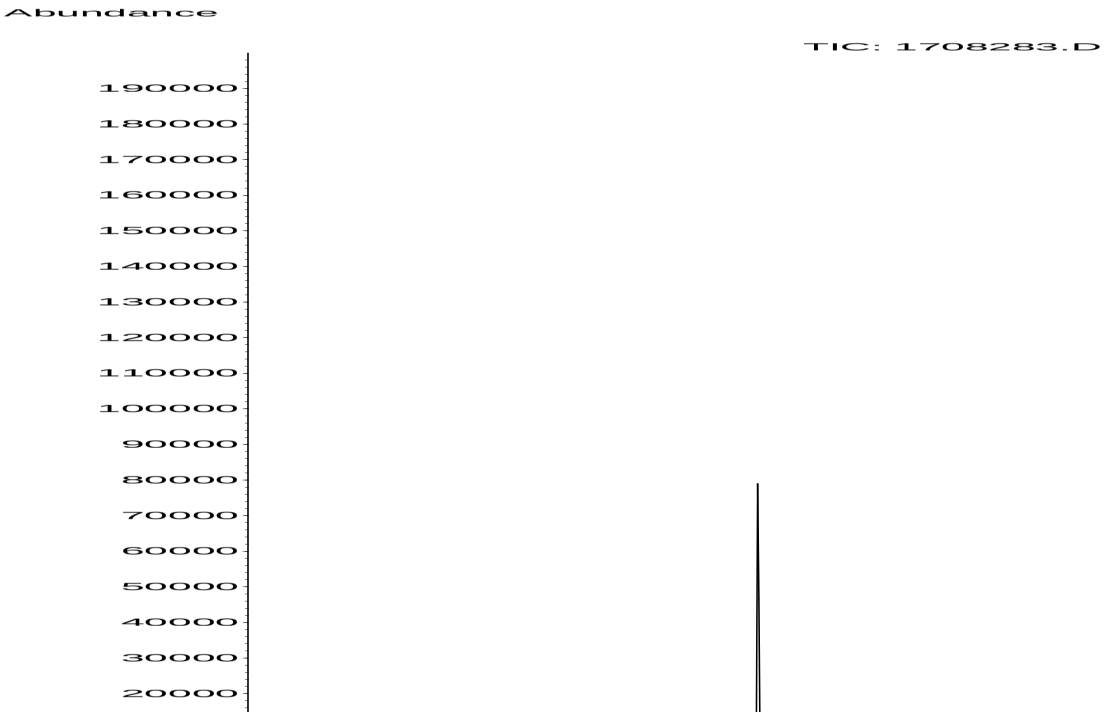

Figure 38: 0.5 ppm PAH after adsorption by 40% Fe_3O_4/MWCNT in 5 minute

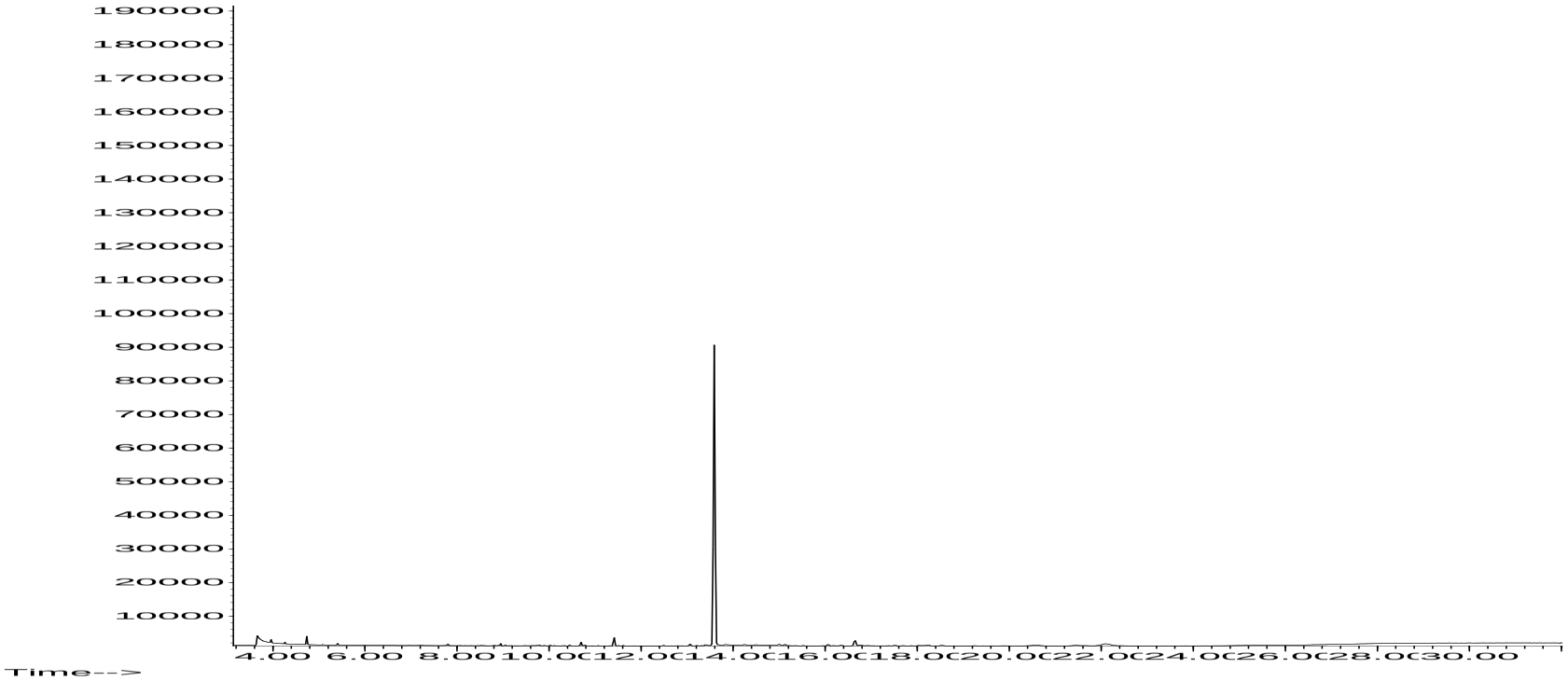

Figure 39: 0.5 ppm PAH after adsorption by 40% Fe_3O_4/MWCNT in24 hours

Information from Data File:
File: C:\MSDCHEM\1\DATA\1708221.D
Operator: eda
Date Acquired: 23 Aug 2017 2:12
Method File: EDAPAH
Sample Name: 10 ppm PAH scan
Misc Info:
Vial Number: 1

Search Libraries: C:\DATABASE\NIST11.L Minimum Quality: 0
C:\DATABASE\wiley7n.L Minimum Quality: 0
C:\DATABASE\ORGANIC.L

Unknown Spectrum: Apex minus start of peak
Integration Events: Chemstation Integrator - autoint1.e

Pk#	RT	Area%	Library/ID	Ref#	CAS#	Qual
1	3.47	3.29	C:\DATABASE\NIST11.L			
			Cyclohexane	1455	000110-82-7	9
			4-Cyclopentene-1,3-diol, trans-	3727	000694-47-3	9
			Cyclohexane	1459	000110-82-7	5
2	3.64	40.19	C:\DATABASE\NIST11.L			
			Cyclohexane	1456	000110-82-7	83
			2-Amino-oxazole	1333	004570-45-0	80
			Cyclohexane	1459	000110-82-7	64
3	3.67	1.18	C:\DATABASE\NIST11.L			
			Ethylidenecyclobutane	1219	001528-21-8	80
			Cyclohexene	1190	000110-83-8	80
			3-Hexyne	1187	000928-49-4	64
4	3.83	1.97	C:\DATABASE\NIST11.L			
			Cyclohexane, methyl-	3342	000108-87-2	91
			Cyclohexane, methyl-	3340	000108-87-2	91
			Cyclohexane, methyl-	3338	000108-87-2	78
5	3.89	0.23	C:\DATABASE\NIST11.L			
			Cyclopentane, ethyl-	3337	001640-89-7	91
			Cyclopentane, ethyl-	3341	001640-89-7	53
			Cyclopentanone, 3-methyl-	3229	001757-42-2	46
6	4.03	0.10	C:\DATABASE\NIST11.L			
			Cyclohexane, methylene-	2885	001192-37-6	91
			Norbornane	2838	000279-23-2	90
			Cyclohexane, methylene-	2883	001192-37-6	72
7	4.32	1.14	C:\DATABASE\NIST11.L			
			5-Hexenal	3133	000764-59-0	64
			3-Cyclohexen-1-ol	3182	000822-66-2	56
			2-Hydroxymethylcyclopentanol (cis)	8194	001883-86-9	43
8	4.47	0.18	C:\DATABASE\NIST11.L			
			Hexanal	3771	000066-25-1	83
			Hexanal	3773	000066-25-1	53
			Cyclohexane, (1,1-dimethylethyl)-	18045	003178-22-1	36
9	4.69	0.14	C:\DATABASE\NIST11.L			
			Cyclopentanecarboxaldehyde	3251	000872-53-7	59
			4-Hexen-3-one	3167	002497-21-4	52
			3-Hexene, 3-methyl-, (Z)-	3376	004914-89-0	50
10	4.73	0.53	C:\DATABASE\NIST11.L			
			7-Oxabicyclo[2.2.1]heptane	3248	000279-49-2	72
			(Z)-Non-3-en-1-yl propyl carbonate	84228	1000372-80-4	53
			Ethyl (Z)-non-3-enyl carbonate	72485	1000373-83-7	53
11	4.96	0.13	C:\DATABASE\NIST11.L			
			Cyclohexane, ethyl-	6669	001678-91-7	91
			Cyclohexane, ethyl-	6668	001678-91-7	91
			Cyclohexane, ethyl-	6667	001678-91-7	91
12	5.33	0.86	C:\DATABASE\NIST11.L			
			7-Oxabicyclo[2.2.1]heptane	3248	000279-49-2	64
			1,2,3,6-Tetrahydropyridine	1302	000694-05-3	64
			Aziridine, 2-methylene-1-(1-met...	3006	055268-35-4	59

13	5.72	0.61	C:\DATABASE\NIST11.L				
			Cyclohexanol	3788	000108-93-0	95	
			Cyclohexanol	3796	000108-93-0	94	
			Cyclohexanol	3798	000108-93-0	91	
14	5.91	0.64	C:\DATABASE\NIST11.L				
			Cyclohexanone	3164	000108-94-1	91	
			Cyclohexanone	3166	000108-94-1	90	
			Cyclohexanone	3163	000108-94-1	90	
15	8.67	3.12	C:\DATABASE\NIST11.L				
			Oxalic acid, dicyclohexyl ester	105359	1000309-30-9	72	
			Oxalic acid, cyclohexyl propyl ...	72317	1000309-30-3	56	
			Oxalic acid, cyclohexyl ethyl e...	60819	1000309-30-2	56	
16	8.94	0.33	C:\DATABASE\NIST11.L				
			3-Ethyl-3-methylheptane	19200	017302-01-1	72	
			Octane, 2,3,6,7-tetramethyl-	38354	052670-34-5	53	
			Undecane, 5-methyl-	38325	001632-70-8	53	
17	9.04	0.11	C:\DATABASE\NIST11.L				
			Dodecane	38318	000112-40-3	90	
			Undecane, 4,7-dimethyl-	48860	017301-32-5	78	
			Decane, 2,3,7-trimethyl-	48887	062238-13-5	72	
18	9.78	0.12	C:\DATABASE\NIST11.L				
			Undecane, 4-methyl-	38326	002980-69-0	68	
			Decane, 3,6-dimethyl-	38343	017312-53-7	68	
			Bacchotricuneatin c	178298	066563-30-2	64	
19	11.40	1.48	C:\DATABASE\NIST11.L				
			Naphthalene	11942	000091-20-3	95	
			Naphthalene	11939	000091-20-3	94	
			Azulene	11938	000275-51-4	91	
20	13.06	0.42	C:\DATABASE\NIST11.L				
			Heptadecane, 8-methyl-	105898	013287-23-5	83	
			Tridecane, 1-iodo-	152416	035599-77-0	72	
			Tetradecane, 4-methyl-	71399	025117-24-2	58	
21	13.57	0.42	C:\DATABASE\NIST11.L				
			1,1'-Bicyclohexyl	35158	000092-51-3	91	
			1,1'-Bicyclohexyl	35159	000092-51-3	91	
			1,1'-Bicyclohexyl	35160	000092-51-3	90	
22	13.86	0.15	C:\DATABASE\NIST11.L				
			Undecane, 4,6-dimethyl-	48869	017312-82-2	64	
			Dodecane, 1-iodo-	140552	004292-19-7	59	
			Dodecane, 2,6,11-trimethyl-	71406	031295-56-4	59	
23	15.25	0.19	C:\DATABASE\NIST11.L				
			Cyclohexylmethylsilane	12394	002096-99-3	38	
			Succinic acid, trans-hex-3-enyl...	186707	1000353-43-4	38	
			Fumaric acid, cis-hex-3-enyl oc...	227151	1000348-87-3	35	
24	16.07	6.95	C:\DATABASE\NIST11.L				
			Biphenylene	25457	000259-79-0	94	
			Biphenylene	25454	000259-79-0	91	
			Acenaphthylene	25458	000208-96-8	90	
25	16.65	7.90	C:\DATABASE\NIST11.L				
			Acenaphthene	27109	000083-32-9	76	
			Acenaphthene	27110	000083-32-9	72	
			Acenaphthene	27112	000083-32-9	64	
26	16.78	0.38	C:\DATABASE\NIST11.L				
			Pentacosane	185533	000629-99-2	78	
			Tridecane, 5-propyl-	83031	055045-11-9	78	
			Heptadecane, 8-methyl-	105898	013287-23-5	72	
27	18.26	8.17	C:\DATABASE\NIST11.L				
			Fluorene	35227	000086-73-7	94	
			Fluorene	35228	000086-73-7	91	
			3-Trifluoromethylbenzhydryl chl...	118744	067240-79-3	64	

28	21.57	9.97	C:\DATABASE\NIST11.L		
			Anthracene	44136	000120-12-7 95
			Phenanthrene	44142	000085-01-8 93
			Phenanthrene	44141	000085-01-8 93
29	21.73	7.39	C:\DATABASE\NIST11.L		
			Phenanthrene	44142	000085-01-8 72
			Anthracene	44136	000120-12-7 72
			Phenanthrene	44143	000085-01-8 72
30	27.87	1.71	C:\DATABASE\NIST11.L		
			Fluoranthene	62827	000206-44-0 96
			Fluoranthene	62828	000206-44-0 95
			Pyrene	62822	000129-00-0 94

Figure 40: Library Search Results from the GC-MS